Counter-Diabatic Driving for Periodically Driven Three-Level Systems

This thesis is submitted in partial fulfillment of the requirements

for the degree of

M.Sc. in Quantum Technology

by

Georgi Aleksandrov

(student ID: 7PH3100031)

Theoretical Physics Department
Faculty of Physics
Sofia University

March 18, 2025

SOFIA UNIVERSITY ST. KLIMENT OHRIDSKI

Approved by

Thesis Supervisor:	Marin Bukov, PhD
Co-advisor:	Assoc. Prof. Dr. Andon Rangelov
Referee:	Prof. Steve Campbell, PhD
defense date:	26.03.2025

Certificate of Originality

*This is to certify that this thesis, entitled "**Counter-Diabatic Driving for Periodically Driven Three-Level Systems**", submitted in partial fulfillment of the requirements for the degree M.Sc. in Quantum Technology at Sofia University, is my own work and contains original results obtained by myself with the support and assistance of my supervisor.*

In particular, I certify that results and ideas obtained by third parties that are described, published, or authored elsewhere, are to a sufficient extent referred to, properly cited, and acknowledged in the thesis, in accordance with the requirements for respecting intellectual property, and the academic ethics and standards.

I am aware that, should plagiarism or scientific misconduct be established, the Thesis Committee reserves the right to reject this thesis, while the Committee for Academic Ethics at the Ministry of Science and Education has the legal right to retroactively revoke the degree conferred.

I declare that the results contained in the present thesis have not been submitted at any other university, institute, or higher-education institution in (partial) fulfillment of the requiements for an academic degree.

Sofia
March 18, 2025

Georgi Aleksandrov
student ID: 7PH3100031
Faculty of Physics
Sofia University

Abstract

Counter-diabatic (CD) driving is a shortcut for adiabatic quantum control. By adding a gauge potential to the time-dependent Hamiltonian, we compensate non-adiabatic transitions.

This thesis investigates CD driving for three-level systems, which exhibit richer physics than two-level systems. Their dynamics are generally unsolvable analytically, so we use a variational method to find gauge potentials.

Floquet theory is related closely to CD driving – the Hamiltonian of a periodic system is a CD-driven Floquet Hamiltonian. Using this, we derive variational Floquet Hamiltonians for specific two- and three-level systems.

Using the $SU(3)$ group properties, we provide the most general parameterization of a gauge potential in three-level systems, corresponding to pure micromotion drives in Floquet theory. Representing $\mathfrak{su}(3)$ algebra elements as vectors with dot, vector, and "star" products, we obtain an exact Kato gauge potential formula and a simplified version for degenerate systems.

Finally, we propose a fully geometric two-qubit quantum gate, evolving solely via the Kato potential.

Контрадиабатично задвижване на квантови системи с три нива

Дипломна работа представена за частично покриване на изискванията за образователно-квалификационна степен

магистър "Квантова информатика"

от

Георги Мирославов Александров

(факултетен номер: 7PH3100031)

Катедра Теоретична Физика
Физически Факултет
Софийски университет „Св. Климент Охридски“

18 март 2025 г.

Одобрена от

ръководител:	д-р Марин Буков
консултант:	доц. дфзн Андон Рангелов
рецензент:	проф. д-р Стийв Кемпбъл
дата на защитата:	26.03.2025

Декларация за оригиналност и автентичност

Аз, ***Георги Мирославов Александров****, студент от Физически Факултет на Софийски университет „Св. Климент Охридски“, декларирам, че представената от мен за защита дипломна работа на тема:* ***„Контрадиабатично задвижване на квантови системи с три нива”****, за присъждане на образователно-квалификационна степен магистър "Квантова информатика" е оригинална разработка и съдържа оригинални резултати, получени при проведени от мен научни изследвания (с подкрепата и/или съдействието на научния ми ръководител).*

Декларирам, че резултатите, които са получени, описани и/или публикувани от други учени, са надлежно и подробно цитирани, при спазване на изискванията за защита на авторското право и на академичната етика и стандарти.

Уведомен/а съм, че в случай на констатиране на плагиатство или недостоверност на представените научни данни, Комисията по защитата е в правото си да я отхвърли, а Комисията по академична етика към Министерство на образованието и науката е в законното си правото да анулира придобитата образователно-квалификационна степен.

Декларирам, че настоящият труд не е представян пред други университети, институти и други висши училища за придобиване на образователна и/или научна степен.

София
18 март 2025 г.

Георги Мирославов Александров
факултетен номер: 7PH3100031
Физически Факултет
Софийски университет „Св. Климент Охридски“

Абстракт

Контрадиабатичното задвижване е пряк път за адиабатичен квантов контрол. Добавянето на калибровъчен потенциал към времезависим хамилтониан компенсира изцяло неадиабатичните преходи.

Дипломната работа разширява контрадиабатичното задвижване за системи от три нива, притежаващи по-богата физиката от системите с две нива. Например, могат да съдържат изродени нива, при което в адиабатичната им еволюция се наблюдава квантова холономия. Тъй като динамиката им в общия случай не е аналитично решима, ние разглеждаме вариационен метод за намиране на калибровъчни потенциали.

Теорията на Флоке за периодично задвижените се оказва тясно свързана с контрадиабатичното задвижване – хамилтонианът на такива системи е контрадиабатично задвижен хамилтониан на Флоке. Използвайки този факт, ние намираме вариационно хамилтониани на Флоке за конкретни примерни системи с две и три нива.

Използвайки свойствата на групата $SU(3)$, даваме най-общата параметризация за калибровъчен потенциал в система от три нива. Във Флоке теорията това са задвижвания без Флоке еволюция. Също така, използваме представяне на елементите на алгебрата $\mathfrak{su}(3)$ като вектори, в които може да се въведе "скаларно" и "векторно произведение", за да получим точна формула за калибровъчния потенциал на Като, както и по-проста точна формула в случаите на дегенерирана система.

Накрая, предлагаме схема за построяването на двукюбитен квантов гейт, който е изцяло геометричен – еволюцията му се дължи само на потенциал на Като.

Acknowledgments

First and foremost, I am infinitely grateful to my advisor, **Marin Bukov, PhD**, who guided me throughout the whole process. He introduced me to all the necessary topics of the thesis, helped whenever I got stuck and nudged me to work enough so that this thesis could emerge. Also, I would like to thank my friends and family for their emotional support, in particular Aleksander Iliev for his timely help.

Contents

List of Figures

List of Tables

List of Algorithms

List of Acronyms

2LS Two-level systems 22

3LS three-level systems 1, 45, 47, 48

4LS four-level system 48

AGP Adiabatic Gauge Potential 1, 6, 8, 10, 13, 22, 25, 26, 34–44, 46, 47, 50

CD Counter-diabatic iii, 1, 3, 8, 11, 13, 15, 22, 47

Chapter 1

Introduction

Modern quantum technology demands rapid and precise control over quantum states. A quantum system can be driven to a target state using adiabatic control [1]. This means that if the Hamiltonian guiding the system evolves *slowly*, the system approximately follows its eigenstate. In practice, quantum systems cannot be completely isolated from the environment. Their natural decoherence gives us a finite time for state preparations, leaving adiabatic control impractical.

Counter-diabatic (CD) driving offers a *shortcut to adiabaticity*. By adding a *gauge potential* to a rapidly evolving Hamiltonian, we achieve the same (except faster) evolution as if the variations of the Hamiltonian were adiabatic.

We focus on Floquet systems because of the recent discoveries [2] connecting them to CD driving. As we explain in detail in Sec. 3.2, it turns out that the periodic Hamiltonian governing the Floquet system can be viewed as the sum of the Floquet Hamiltonian and a counter-diabatic term. This allows us to recycle the variational methods for searching for gauge potentials in Floquet theory, where we are concerned with obtaining a Floquet Hamiltonian for a given system.

While CD driving has been extensively studied in two-level systems, its application to multi-level and periodically driven systems remains an open frontier. In this thesis, we expand our knowledge of CD driving by tackling three-level systems (3LS). Three level systems offer richer dynamics. They show a lot of the strange properties occurring in multi-level systems. We are particularly interested in investigating systems with degenerate *energy* levels. Such systems, subject to adiabatic evolution, can move freely within the degenerate subspace. This gives rise to a *holonomic* evolution that we aim to investigate.

The remainder of this thesis is structured as follows: Chapter 2 introduces the theoretical foundation of CD driving, detailing the role of gauge potentials in achieving transitionless evolution. Chapter 3 provides an overview of Floquet theory and its relevance to driven quantum systems. Chapter 4 presents some necessary instruments to compute gauge potentials, including variational approaches. Chapter 5 applies these instruments to simpler, two-level systems. preparing us for the challenges of 3LS. We make numerical simulations for concrete two-level systems. Then, in Chapter 6, we delve into the theory behind 3LS. To do this effectively, we discuss the $SU(3)$ group and respective algebra. Then, we give a parametrization of the most general form of the Adiabatic Gauge Potential (AGP) and a simplified parametrization specifically useful for Floquet systems.

Then, we give formulae for computing Kato gauge potentials in the degenerate and non-degenerate three level systems, concluding the theoretical results of the thesis. Next, we move on to numerical experiments in Chapter 7. Finally, Chapter 8 summarizes our findings and outlines potential future directions of research.

Chapter 2

Counter-Diabatic Driving

This chapter lays the theoretical foundation for CD driving. We begin by stating the adiabatic theorem. We show how a quantum system remains in an instantaneous eigenstate if the Hamiltonian's parameters change slowly. We then introduce the concept of Berry phase for adiabatic evolution and generalize it to a holonomy matrix in degenerate systems. If the evolution of the Hamiltonian is faster, we show that we can prevent transitions between states using a *gauge potential*. We discuss properties of gauge potential and focus on the parallel-transport *Kato gauge potential*. This chapter establishes why these gauge potentials are important: they are the key to implementing shortcuts to adiabaticity, enabling fast quantum operations without loss of fidelity. The concepts introduced in this chapter are fundamental for the rest of the thesis, where we will find or use gauge potentials in particular systems.

2.1 Adiabatic Theorem

If we evolve a quantum system from its eigenstate with a *slowly* changing Hamiltonian, it will remain in the instantaneous eigenstate. This result is known as the adiabatic theorem.

To state the theorem formally, consider a Hamiltonian with a time-dependent parameter $\lambda(t)$

$$H = H(\lambda(t)). \tag{2.1}$$

The **instantaneous eigenstates** are the eigenstates $|\psi_n(\lambda)\rangle$ for a fixed value of the parameter $\lambda(t)$:

$$H(\lambda)\,|\psi_n(\lambda)\rangle = E_n(\lambda)\,|\psi_n(\lambda)\rangle\,. \tag{2.2}$$

In general, they differ from the time-evolved states

$$|\psi_n(\lambda(t))\rangle \neq \mathcal{T}e^{-i\int_0^t dt' H(\lambda(t'))}\,|\psi_n(\lambda(0))\rangle\,. \tag{2.3}$$

Note that the instantaneous eigenstates are orthonormal for a fixed time t, but $\langle\psi_m(\lambda_1)|\psi_n(\lambda_2)\rangle \neq 0$ for $\lambda_1 \neq \lambda_2$.

The theorem states that the evolved state is close to the instantaneous eigenstate if λ changes slower than the gap Δ between the instantaneous eigenstates. More precisely,

the condition is

$$\left|\frac{\dot{\lambda}}{\Delta(\lambda)}\right| |\langle\psi_m(\lambda)|\partial_\lambda H|\psi_n(\lambda)\rangle| \ll 1, \qquad \forall\lambda, \forall m, n, \tag{2.4}$$

where $\Delta(\lambda) = E_m(\lambda) - E_n(\lambda)$ is the energy gap between the instantaneous eigenstates $|\psi_m\rangle$ and $|\psi_n\rangle$. As we can see, this condition implies that we have small enough $\dot{\lambda}$ (slow changes of the parameter) and large enough Δ (band gap).

Proof

To prove the theorem, we use time-dependent perturbation theory.

If the Hamiltonian did not depend on time, the solution to Schrödinger's equation

$$i\partial_t |\Psi(t)\rangle = H |\Psi(t)\rangle \tag{2.5}$$

would be

$$|\Phi(t)\rangle = \sum_n c_n e^{-itE_n} |\phi_n\rangle , \tag{2.6}$$

where $|\phi_n\rangle$ are the eigenstates of the time-independent Hamiltonian, and E_n are the corresponding energies,

$$H |\phi_n\rangle = E_n |\phi_n\rangle . \tag{2.7}$$

Similarly, for the time-dependent Hamiltonian, we expand the solutions in the basis of the instantaneous eigenstates $|\psi_n\rangle$, with time-dependent coefficients $c_n(t)$:

$$|\Psi(t)\rangle = \sum_n c_n(t) e^{i\theta_n(t)} |\psi_n(\lambda(t))\rangle, \tag{2.8}$$

where $\theta_n(t) = -\int_0^t dt' E_n(t')$ is called the **dynamical phase** of the wave function. Note that we can always transfer phases to and from c_n. As we will see, $c_n(t)$ contains an additional Berry phase. The dynamical phase θ is defined in such a way as to match the time-independent phase $E_n t$.

We now substitute the expansion (2.8) to (2.5) and get

$$\begin{aligned} i\sum_n (\dot{c}_n|\psi_n\rangle + c_n|\dot{\psi}_n\rangle + c_n|\psi_n\rangle i\dot{\theta}_n) e^{i\theta_n} &= \sum_n c_n(t) E_n(t) e^{i\theta_n(t)} |\psi_n\rangle \\ i\sum_n (\dot{c}_n|\psi_n\rangle + c_n\dot{\lambda}|\partial_\lambda\psi_n\rangle - c_n|\psi_n\rangle i E_n(t)) e^{i\theta_n(t)} &= \sum_n c_n(t) E_n(t) e^{i\theta_n(t)} |\psi_n\rangle \\ i\sum_n (\dot{c}_n|\psi_n\rangle + c_n\dot{\lambda}|\partial_\lambda\psi_n\rangle) e^{i\theta_n(t)} &= 0. \end{aligned} \tag{2.9}$$

We multiply by $\langle\psi_m|$ to get

$$i\dot{c}_m(t) e^{i\theta_n(t)} + i\sum_n c_m(t)\dot{\lambda}\langle\psi_m|\partial_\lambda|\psi_n\rangle e^{i\theta_n(t)} = 0. \tag{2.10}$$

In the generic case, the off-diagonal elements $\langle\psi_m|\partial_\lambda|\psi_n\rangle$, $n \neq m$ are responsible for transitions $|\psi_n\rangle \to |\psi_m\rangle$. In the case of small $\dot{\lambda}$, $n \neq m$ terms are negligible. To see this more precisely, we differentiate the equation

$$\langle\psi_m(\lambda)|H(\lambda)|\psi_n(\lambda)\rangle = 0. \tag{2.11}$$

$$
\begin{aligned}
0 &= \langle \partial_\lambda \psi_m | H | \psi_n \rangle + \langle \psi_m | \partial_\lambda H | \psi_n \rangle + \langle \psi_m | H | \partial_\lambda \psi_n \rangle \\
0 &= E_n \langle \partial_\lambda \psi_m | \psi_n \rangle + \langle \psi_m | \partial_\lambda H | \psi_n \rangle + E_m \langle \psi_m | \partial_\lambda \psi_n \rangle \\
0 &= (E_m - E_n) \langle \psi_m | \partial_\lambda \psi_n \rangle + \langle \psi_m | \partial_\lambda H | \psi_n \rangle,
\end{aligned} \tag{2.12}
$$

$$
\langle \psi_m | \partial_\lambda | \psi_n \rangle = \frac{\langle \psi_m | \partial_\lambda H | \psi_n \rangle}{E_n - E_m}. \tag{2.13}
$$

Comparing the expression with (2.4), we see that the $n \neq m$ terms are indeed negligible. This turns Eq. (2.10) in the transitionless differential equation

$$
\dot{c}_m \approx i c_m \dot{\lambda} \langle \psi_m | i \partial_\lambda | \psi_m \rangle, \tag{2.14}
$$

whose solution is

$$
c_m(t) \approx c_m(0) e^{i\gamma_m(t)}, \tag{2.15}
$$

where

$$
\gamma_m(t) = \int_0^t dt' \dot{\lambda} \langle \psi_m(\lambda) | i \partial_\lambda | \psi_m(\lambda) \rangle = \int_0^{\lambda(t)} d\lambda \langle \psi_m(\lambda) | i \partial_\lambda | \psi_m(\lambda) \rangle
$$

is called **Berry phase**, and the integrand

$$
A_m(\lambda) = \langle \psi_m | i \partial_\lambda | \psi_m \rangle \tag{2.16}
$$

is called **Berry connection**.

Finally, if we evolve the Hamiltonian from an initial state $|\psi_m(0)\rangle$, meaning that $c_m(0) = 1; c_n(0) = 0 \quad \forall n \neq m$, we would end up at

$$
|\Psi(t)\rangle \approx c_m(0) e^{i\theta_m(t)} e^{i\gamma_m(t)} |\psi_m\rangle, \tag{2.17}
$$

accumulating a dynamical phase θ_m and a Berry phase γ_m.

2.2 Berry Phase and Holonomy

We revise the adiabatic theorem proved in 2.1 for the case when the Hamiltonian has degenerate energy levels. Up to Eq. (2.10), there is no need for the energy levels to be different. For each degeneracy $\theta_n = \theta$, we can only neglect the different-energy terms $E_k \neq E_n$ in the differential equation. This leaves us with

$$
\dot{c}_m = i \sum_n \langle \psi_m | i \partial_t | \psi_n \rangle c_n \tag{2.18}
$$

This equation can be formally solved as

$$
\vec{c}(t) = \mathcal{T} e^{i \int_0^t dt' A(t')} \vec{c}(0) = W \vec{c}(0), \tag{2.19}
$$

where A is a matrix of Berry connections,

$$
A_{mn} = \langle \psi_m | i \partial_t | \psi_n \rangle, \tag{2.20}
$$

and W is called **holonomy matrix**. Its dimension is equal to the degree of the degeneracy. In case of degenerate energy levels, the adiabatic theorem does not hold – the state can evolve among the degenerate levels.

2.3 Gauge Potential

When changing the coordinate system, the Hamiltonian transforms similarly to a general hermitian operator. However, it also obtains a gauge potential, similarly to the fictitious forces emerging from non-inertial transformations in classical physics.

Let U be a unitary transformation from $|\psi\rangle$ ("lab frame") to $|\tilde{\psi}\rangle$ ("moving frame"), such that

$$|\tilde{\psi}\rangle = U^\dagger |\psi\rangle \,. \tag{2.21}$$

In the lab frame,

$$i\partial_t |\psi\rangle = \hat{H} |\psi\rangle \,. \tag{2.22}$$

Substituting $|\psi\rangle = U|\tilde{\psi}\rangle$, we get

$$\begin{aligned} i\partial_t \left(U|\tilde{\psi}\rangle\right) &= \hat{H}U|\tilde{\psi}\rangle \\ i(\partial_t U)|\tilde{\psi}\rangle + iU\partial_t|\tilde{\psi}\rangle &= \hat{H}U|\tilde{\psi}\rangle \\ i\partial_t|\tilde{\psi}\rangle &= U^\dagger HU|\tilde{\psi}\rangle - iU^\dagger(\partial_t U)|\tilde{\psi}\rangle \\ i\partial_t|\tilde{\psi}\rangle &= \tilde{H}_{\text{moving}}|\tilde{\psi}\rangle. \end{aligned} \tag{2.23}$$

The dynamics in the new frame are governed by a **moving frame Hamiltonian** $\tilde{H}_{\text{moving}}$, which can be represented as

$$\tilde{H}_{\text{moving}} = \tilde{H} - \tilde{\mathcal{A}}, \tag{2.24}$$

where

$$\tilde{H} = U^\dagger HU \tag{2.25}$$

is the rotated Hamiltonian from the static frame and

$$\tilde{\mathcal{A}} = iU^\dagger \partial_t U \tag{2.26}$$

is the additional **gauge potential**. If we rotate the gauge potential back to the lab frame, we get

$$\mathcal{A}_t = U\tilde{\mathcal{A}}_t U^\dagger = i\partial_t U U^\dagger. \tag{2.27}$$

The dynamical Adiabatic Gauge Potential (AGP) with respect to a parameter-dependent transformation $U(\lambda)$ is defined as

$$\mathcal{A}_\lambda^U = i\partial_\lambda U U^\dagger. \tag{2.28}$$

To get a better intuition about this gauge potential, we draw an analogy with Newtonian dynamics. In classical mechanics, Newton's laws are valid in inertial reference frames. If we switch to a non-inertial reference frame, we need to "fix" Newton's second law $\vec{F} = m\vec{a}$ by adding centrifugal and Coriolis force.

Similarly, in quantum mechanics, if we change the reference frame, to fix Schrodinger's equation, we add a gauge potential to the Hamiltonian. Our quantum particles in a rotating reference frame experience the fields from the lab Hamiltonian H and "fictitious energy" from the gauge potential.

2.3.1 Properties of the Gauge Potential

The gauge potential is the generator of the unitary transformation:

$$U(\lambda) = \mathcal{P} \exp\left(-i \int_0^\lambda \mathcal{A}^U(\lambda') d\lambda'\right). \tag{2.29}$$

We can see that by taking

$$\begin{aligned} U(\lambda + d\lambda) &= e^{-i\mathcal{A}_\lambda^U d\lambda} U(\lambda) \approx \left(1 - i\mathcal{A}_\lambda^U d\lambda\right) U(\lambda) \\ dU &= -i\mathcal{A}_\lambda^U d\lambda U \\ dUU^\dagger &= -i\mathcal{A}_\lambda^U d\lambda \\ i\partial_\lambda UU^\dagger &= \mathcal{A}_\lambda^U. \end{aligned} \tag{2.30}$$

The gauge potential is Hermitian.

$$\begin{aligned} UU^\dagger &= 1 \\ \partial_\lambda(UU^\dagger) &= 0 \\ \partial_\lambda UU^\dagger + U\partial_\lambda U^\dagger &= 0 \\ i\partial_\lambda UU^\dagger &= -iU\partial_\lambda U^\dagger \\ \mathcal{A}_\lambda^U &= \mathcal{A}_\lambda^{U\dagger}. \end{aligned} \tag{2.31}$$

The gauge potential acts as a derivative operator on states which are static in the rotated frame.

Let the transformation U send the states $|\psi_n(t)\rangle$ to $|e_n\rangle = \text{const}$.

$$i\partial_\lambda |\psi_n\rangle = i\partial_\lambda(U|e_n\rangle) = i\partial_\lambda U |e_n\rangle = i\partial_\lambda UU^\dagger |\psi_n\rangle = \mathcal{A}_\lambda^U |\psi\rangle_n. \tag{2.32}$$

This gives us another interesting property. Suppose we find a transformation that diagonalizes a time-dependent Hamiltonian. The corresponding gauge potential acts as a derivative operator on the instantaneous eigenstates. Therefore, *the diagonal elements of the gauge potential are the Berry connections*:

$$A_n = i\langle\psi_n(\lambda)|\partial_\lambda|\psi_n(\lambda)\rangle. \tag{2.33}$$

2.3.2 Counter-Diabatic Driving

Consider a quantum system with a non-adiabatic Hamiltonian $H(\lambda(t))$. It will not remain in its eigenstate on its own. To cancel the non-adiabatic transitions, we can add a driving term $\dot{\lambda}\mathcal{A}_\lambda^U = i\dot{U}U^\dagger$, where U diagonalizes H. The counter-diabatically driven Hamiltonian takes the form

$$H_{CD} = H + \dot{\lambda}\mathcal{A}_\lambda^U. \tag{2.34}$$

To see that the system remains in its eigenstate, we transform the Hamiltonian to the moving frame:

$$\tilde{H}_{\text{moving}} = U^\dagger(H + i\dot{U}U^\dagger)U - iU^\dagger\dot{U} = U^\dagger HU, \tag{2.35}$$

where $U^\dagger HU$ is now a diagonal Hamiltonian. This means the system will indeed follow the instantaneous eigenstates of H.

As the $U^\dagger HU$ is diagonal, the evolved states accumulate only dynamic phases. In contrast, the evolution with an adiabatic Hamiltonian generates dynamic and Berry phases, as in Eq. (2.17).

Counter-diabatic driving is a shortcut to adiabaticity [3]

Adiabatic protocols are actively used in quantum computers [4]. For example, the quantum adiabatic algorithm is a way to find the ground state of a Hamiltonian H_{target}. The system is prepared the system in the ground state of a simple Hamiltonian $H(0)$. Then, the Hamiltonian evolves as $H(\lambda)$ to a new Hamiltonian $H(\lambda_{\text{final}}) = H_{\text{target}}$. If λ changes adiabatically, the evolved state follows the instantaneous ground eigenstate, finally reaching the ground state of H_{target}. The problem is that adiabatic evolution takes a lot of time, which leads to decoherence. The *shortcut* is that we can use a faster CD driven Hamiltonian $H_{CD} = H(\lambda) + \dot{\lambda}\mathcal{A}_\lambda$, where the CD term will keep the system at the instantaneous eigenstates of $H(\lambda)$ despite the quicker evolution. This means that the system will be prepared in the desired state faster, e.g. within coherence time.

2.4 Kato Gauge Potential

The AGP that permits CD driving is in fact defined up to a *gauge freedom*. So far, we have discussed the *dynamical-gauge* AGP $\mathcal{A}^U$. Suppose we use an arbitrary gauge $\mathcal{A}^U + UDU^\dagger$, where D is diagonal. The moving Hamiltonian $\tilde{H}_{\text{moving}} = U^\dagger HU + D$ would still be diagonal. The "simplest" potential we can use would have no diagonal part. It is called the **Kato** AGP.

By taking advantage of Eq. (2.13), we can define the Kato AGP as

$$\mathcal{A}^K_\lambda = i \sum_{m \neq n} \frac{\langle \psi_m | \partial_\lambda H | \psi_n \rangle}{E_n - E_m} |\psi_m\rangle \langle \psi_n| \,. \tag{2.36}$$

There is also an alternative definition that does not rely explicitly on the energies and the basis:

$$\mathcal{A}^K_\lambda = \frac{1}{2} \sum_\alpha [i\partial_\lambda \Pi_\alpha, \Pi_\alpha] \tag{2.37}$$

Proof that both definitions are equivalent

First, recall that the projector has the form

$$\Pi_\alpha = |\psi_\alpha\rangle \langle \psi_\alpha| \tag{2.38}$$

and the eigenstates are constant in the moving basis, therefore

$$U^\dagger \Pi_\alpha U = |e_\alpha\rangle \langle e_\alpha| = \text{const.} \tag{2.39}$$

By differentiating this identity, we get

$$U^\dagger \partial_\lambda \Pi_\alpha U = -\partial_\lambda U^\dagger \Pi_\alpha U - U^\dagger \Pi_\alpha \partial_\lambda U. \tag{2.40}$$

Multiplying Eq. (2.40) on the right and on the left by $U^\dagger \Pi_\alpha U$, we get respectively

$$\begin{aligned} U^\dagger \partial_\lambda \Pi_\alpha \Pi_\alpha U &= -\partial_\lambda U^\dagger \Pi_\alpha^2 U - U^\dagger \Pi_\alpha \partial_\lambda U U^\dagger \Pi_\alpha U, \\ U^\dagger \Pi_\alpha \partial_\lambda \Pi_\alpha U &= -U^\dagger \Pi_\alpha U \partial_\lambda U^\dagger \Pi_\alpha U - U^\dagger \Pi_\alpha^2 \partial_\lambda U \end{aligned} \tag{2.41}$$

Subtracting the above equations, we get

$$U^\dagger[i\partial_\lambda \Pi_\alpha, \Pi_\alpha]U = -i\partial_\lambda U^\dagger \Pi_\alpha U + iU^\dagger \Pi_\alpha \partial_\lambda U - 2U^\dagger \Pi_\alpha \mathcal{A}_\lambda^U \Pi_\alpha U, \tag{2.42}$$

where $\mathcal{A}_\lambda^U = -iU\partial_\lambda U^\dagger = i\partial_\lambda U U^\dagger$ is the adiabatic gauge potential, and $\Pi_\alpha^2 = \Pi_\alpha$ for the projector. If we rotate this equation by multiplying U on the left and $U^\dagger$ on the right, we get

$$[i\partial_\lambda \Pi_\alpha, \Pi_\alpha] = \mathcal{A}_\lambda^U \Pi_\alpha + \Pi_\alpha \mathcal{A}_\lambda^U - 2\Pi_\alpha \mathcal{A}_\lambda^U \Pi_\alpha. \tag{2.43}$$

Notice

$$\Pi_\alpha \mathcal{A}_\lambda^U \Pi_\alpha = \langle \psi_\alpha | \mathcal{A}_\lambda^U | \psi_\alpha \rangle \, |\psi_\alpha\rangle \langle \psi_\alpha| \tag{2.44}$$

are the diagonal elements of the adiabatic gauge potential, and $\sum_\alpha \Pi_\alpha = \mathbf{1}$, which leads to

$$\frac{1}{2}\sum_\alpha [i\partial_\lambda \Pi_\alpha, \Pi_\alpha] = \mathcal{A}_\lambda^U - \mathrm{diag}(\mathcal{A}_\lambda^U) = \mathcal{A}_\lambda^K. \tag{2.45}$$

Kato gauge potential for degenerate Hamiltonian

Suppose we have a degenerate energy level E_α. For all energy levels, Eq. (2.13) does not yield any diagonal matrix elements. For the degenerate energy levels, all "blocks" of matrix elements $\langle \psi_{\alpha_i} | \mathcal{A}_\lambda^K | \psi_{\alpha_j} \rangle$ are also zero.

Looking at the projectors, we can observe the same behaviour. A degenerate projector has the form

$$\Pi_{\alpha_{12}} = |\psi_{\alpha_1}\rangle \langle \psi_{\alpha_1}| + |\psi_{\alpha_2}\rangle \langle \psi_{\alpha_2}| = U I_\alpha U^\dagger, \tag{2.46}$$

where $I_\alpha = \text{const}$. All the steps leading to the identity (2.43) still hold. Then,

$$\langle \psi_{\alpha_1} | [i\partial_\lambda \Pi_\alpha, \Pi_\alpha] | \psi_{\alpha_2} \rangle = \left\langle \psi_{\alpha_1} | \mathcal{A}_\lambda^U + \mathcal{A}_\lambda^U - 2\mathcal{A}_\lambda^U | \psi_{\alpha_2} \right\rangle = 0, \tag{2.47}$$

where $\Pi_\alpha |\psi_{\alpha_2}\rangle = |\psi_{\alpha_2}\rangle$ and $\langle \psi_{\alpha_1}| \Pi_\alpha = \langle \psi_{\alpha_1}|$. The other commutator terms also give zero in the degeneracy block:

$$\left\langle \psi_{\alpha_1} | \mathcal{A}_\lambda^U \Pi_\beta + \Pi_\beta \mathcal{A}_\lambda^U - 2\Pi_\beta \mathcal{A}_\lambda^U \Pi_\beta | \psi_{\alpha_2} \right\rangle = 0, \tag{2.48}$$

because $\Pi_\beta |\psi_{\alpha_2}\rangle = 0$ and $\langle \psi_{\alpha_1}| \Pi_\beta = 0$.

Counter-diabatic Kato driving

A Hamiltonian that is driven counter-diabatically using the Kato gauge potential takes the form

$$H_{CD} = H + \dot{\lambda} \mathcal{A}_\lambda^K. \tag{2.49}$$

Suppose the Hamiltonian diagonalizes to $U^\dagger H U = D$, while the Berry connections are $A_n = \langle \psi_n | \mathcal{A}_\lambda^U | \psi_n \rangle$. For now, we assume there are no degeneracies. In the moving frame, this Hamiltonian takes the form

$$\tilde{H}_{\text{moving}} = U^\dagger (H + \dot{\lambda} \mathcal{A}_\lambda^K) U - U^\dagger \dot{\lambda} \mathcal{A}_\lambda^U U = D + \sum_n \dot{\lambda} A_n |\psi_n\rangle\langle\psi_n|. \tag{2.50}$$

When looking at the evolution of the eigenstates in the rotating reference frame, we see two diagonal Hamiltonians contributing to the evolution. Both of them do not lead to

transitions between the eigenstates. Evolution under D accumulates dynamical phases, while evolution with the Berry connections accumulates Berry phases.

If we evolve the system only using the Kato AGP, we would only accumulate Berry phases:

$$\tilde{\mathcal{A}}^K_{\lambda\ m} = \sum_n \dot{\lambda} A_n |\psi_n\rangle\langle\psi_n|. \tag{2.51}$$

In case of degenerate energy levels, the Berry phases in the degenerate subspace must be replaced by a holonomy matrix. The evolution achived by adding a Kato AGP will contain holonomic transitions between eigenstates.

Chapter 3

Floquet Theory

This chapter introduces Floquet theory, which describes quantum systems under periodic driving. We state the Floquet theorem. Then, we discuss the Floquet gauge potential [5], as well an alternative decomposition with a Kato gauge potential [6]. This chapter shows that the tools of CD driving can be carried over to periodically driven systems, which is crucial since periodic drives are widely used in quantum simulators and qubit control.

A Floquet system is a system with time-dependent periodic Hamiltonian

$$H(t) = H(t+T). \tag{3.1}$$

For a generic time-dependent Hamiltonian, it is difficult to solve the Schrödinger equation

$$i\partial_t \left|\psi(t)\right\rangle = H(t)\left|\psi(t)\right\rangle. \tag{3.2}$$

Formally the solution to the evolution operator is a time-ordered exponent,

$$\begin{aligned} U(t,t_0) &= \mathcal{T}\exp\left(-i\int_{t_0}^{t} dt' H(t')\right) \\ &:= \lim_{N\to\infty} e^{-i\Delta t H(N\Delta t)} e^{-i\Delta t H((N-1)\Delta t)} \cdots e^{-i\Delta t H(\Delta t)} \\ &= \lim_{N\to\infty} \prod_{n=1}^{N} e^{-i\Delta t H(n\Delta t)}, \end{aligned} \tag{3.3}$$

where $\Delta t = (t-t_0)/N$.

3.1 Floquet Theorem

The Floquet theorem states that the evolution of a periodic Hamiltonian $H(t) = H(t+T)$ can be decomposed as

$$U(t,0) = P(t)e^{-itH_F}, \tag{3.4}$$

where the function $P(t+T) = P(t)$ is a periodic operator called **micromotion operator**, and H_F is a constant Hamiltonian called **Floquet Hamiltonian**. The Floquet Hamiltonian governs the stroboscopic, long-term behavior of the driven system. Note that $P(0) = \mathbf{1}$ as $U(0,0) = \mathbf{1}$.

The physical meaning of the theorem is that there exists a rotating frame with a constant Hamiltonian H_F. The matrix $P(t)$ transforms the rotating frame to the lab frame. Indeed, we can add $P^\dagger(0) = \mathbf{1}$ to the right of(3.4) to get

$$\mathcal{T}\exp\left(-i\int_0^t H(t')dt'\right) = P(t)e^{-itH_F}P^\dagger(0), \tag{3.5}$$

meaning that

$$H(t) = P(t)H_F P^\dagger(t) + i\partial_t P(t)P^\dagger(t). \tag{3.6}$$

We can define a **Floquet unitary matrix** as

$$U(T,0) = e^{-iTH_F} = U_F. \tag{3.7}$$

We can formally obtain the Floquet unitary as a time-ordered exponent (3.3). Then, the Floquet Hamiltonian is a matrix logarithm of the Floquet unitary.

The matrix logarithm is not unique. Therefore, the Floquet Hamiltonian is defined up to a gauge freedom, giving us different **quasi-energies**.

This phenomenon has an analogue in solid state physics. If we substitute time with space, Floquet's theorem corresponds to the Bloch theorem – spatially periodic Hamiltonians produce spatially periodic wave functions. There, the particle's momentum is defined up to addition with a reciprocal lattice vector, giving us different *Brillouin zones*.

We define the **Floquet zone** as the zone where the Floquet Hamiltonian has eigenenergies in the range

$$E \in \left[-\frac{\omega}{2}, \frac{\omega}{2}\right), \tag{3.8}$$

where

$$\omega = \frac{2\pi}{T} \tag{3.9}$$

is the driving frequency of the system. Then, a Floquet Hamiltonian with quasi-energy E is equivalent to all other Floquet Hamoltonians with corresponding quasi-energy $E + k\omega, k \in \mathbb{Z}$.

3.2 Floquet Gauge Potential

Let us decompose the evolution similarly to (3.4), starting at $t = t_0$ instead of $t = 0$:

$$U(t,t_0) = P(t,t_0)e^{-i(t-t_0)H_F[t_0]}. \tag{3.10}$$

We can obtain a valid micromotion operator by setting $P(t,t_0) = P(t)P^\dagger(t_0)$, with a Floquet Hamiltonian

$$H_F[t_0] = P(t_0)H_F P^\dagger(t_0). \tag{3.11}$$

Indeed, if we plug this ansatz in (3.6), we get

$$H(t) = P(t,t_0)H_F[t_0]P^\dagger(t,t_0) + i\partial_t P(t,t_0)P^\dagger(t,t_0). \tag{3.12}$$

Note that $H_F[t_0]$ is just a rotated version of H_F. This means $H_F[t_0]$ has the same eigenenergies for any initial time t_0. Also, the micromotion operators starting at different times are generated by the same operator,

$$i\partial_t P(t,t_0)P^\dagger(t,t_0) = i\partial_t P(t)P^\dagger(t) = \mathcal{A}_F(t), \tag{3.13}$$

which we call **Floquet gauge potential**.

During our analysis of gauge potentials in Floquet systems, we will restrict ourselves to gauge potentials with respect to time. This means that from the AGP defined in Eq. (2.28), we will default to $\lambda = t$ and omit the index t. Similarly, we also set $\lambda = t$ from the Kato AGP defined in (2.36) or Eq. (2.37) and we will write it as $\mathcal{A}_K$.

By substituting (3.11), (3.13) in (3.6), we get

$$H(t) = H_F[t] + \mathcal{A}_F(t). \tag{3.14}$$

The Floquet gauge potential performs a Counter-diabatic driving from the Floquet Hamiltonian $H_F[t]$ to the lab frame Hamiltonian $H(t)$ [6]. Here, $H_F[t]$ is viewed as a time-dependent operator, while, $H_F[t_0]$ is a constant Hamiltonian for a fixed initial time t_0.

By knowing the gauge potential, we can reconstruct the micromotion operator,

$$P(t) = \mathcal{T} \exp\left(-i \int_0^t dt' \mathcal{A}_F(t')\right), \tag{3.15}$$

where we used the fact that $P(0) = \mathbf{1}$.

The time-dependent operator $H_F[t]$, due to having constant eigenenergies, always lies in a subspace of all possible Hamiltonians. This subspace is called orbit and is discussed with more details in Sec. 6.1.1

Kato Hamiltonian and Kato Gauge potential

Unlike the Floquet decomposition, there is a unique decomposition of the evolution, using the Kato gauge potential [6]:

$$H(t) = H_K(t) + \mathcal{A}_K(t). \tag{3.16}$$

Again, $H(t)$ obtained by a CD driving. As $\mathcal{A}_K$ is the fixed Kato gauge potential, H_K is a uniquely defined Hamiltonian, which we call "*Kato Hamiltonian*".

This decomposition has some differencies in comparison to the standard Floquet decomposition. The Kato Hamiltonian H_F need not have constant eigenenergies, unlike $H_F[t]$.

Also, the Floquet AGP $\mathcal{A}_F$ is the generator of the *periodic* micromotion $P(t)$ (cf. Eq. (3.15)). However, the time-ordered exponent of $\mathcal{A}_K$,

$$U(t) = \mathcal{T} \exp\left(-i \int_0^t dt' \mathcal{A}_K(t')\right), \tag{3.17}$$

is no longer a necessarily periodic operator such as the micromotion operator. Physically, this time-ordered exponent is the evolution of a system driven only by the Kato AGP. This is classified in the next subsection as a pure geometric drive.

3.2.1 Pure Micromotion and Pure Geometric Drive

In the decomposition (3.14), we notice two special families of drivings. In the case $\mathcal{A}_F = 0$, $H = H_F$, meaning that the system is already static. The more interesting case is $H_F = 0$. In this case, $H(t) = \mathcal{A}_F(t)$, which is a *pure micromotion drive*.

This drive will generate only a micromotion evolution. To derive the general form of a pure micromotion drive, we can compute

$$\mathcal{A}_F(t) = i\dot{P}P^\dagger, \tag{3.18}$$

where P is a unitary operator which obeys the periodic constraint $P(T+t) = P(t)$ and $P(0) = \mathbf{1}$. We parametrize such unitary matrices and corresponding gauge potentials for two and three level systems in Sec. 5.2 and Sec. 6.2.

From the Kato decomposition (3.16), we can obtain another interesting family of drives – *pure geometric drive*. This decomposition will be important for constructing geometric quantum gates, like the CZ gate in Sec. 7.3. This time, we set $H_K = 0$. The Hamiltonian now takes the form

$$H(t) = \mathcal{A}_K(t) + 0 = \mathcal{A}_F(t) + H_F[t]. \tag{3.19}$$

According to Floquet theorem, the evolution over one period takes the form

$$U(T,0) = \mathcal{T}\exp\left(-i\int_0^T \mathcal{A}_K(t')dt'\right) = e^{-iTH_F}. \tag{3.20}$$

On the other hand, evolution from an eigenstate by a Kato driving produces only Berry phases:

$$\gamma(t) = \int_0^t ds\langle u_F[s]|i\partial_s|u_F[s]\rangle, \tag{3.21}$$

where $|u_F[t]\rangle$ are the eigenstates of the Floquet Hamiltonian. Over one period, $\gamma = \varepsilon_F T$.

Chapter 4

Methods for Finding Gauge Potentials

This chapter gives us tools to derive or approximate the gauge potentials introduced earlier. First, in Sec. 4.1, we introduce vector and star products within the $\mathfrak{su}(n)$ Lie algebra, a convenient formalism to manipulate commutators and solve for gauge potentials, specifically when finding closed form of the Kato gauge potential in Sec. 5.1 and Sec. 6.4.

Then, Sec. 4.2 presents approximate methods for finding $\mathcal{A}_\lambda$. We highlight the **least action principle** approach by Sels and Polkovnikov [7], which variationally finds an approximation to the adiabatic gauge potential by minimizing an action functional. In Sec. 4.2.2 we present the modification that adapts the least action principle to Floquet systems [2].

In Sec. 4.2.3, we delve into the specifics of computing the gradients in the least action principle for a Fourier-type ansatz, equipping the reader with the ability to perform the variational principle on their own. Eventually, in Sec. 4.2.3, we share some computational tricks that can speed up the gradient descent process.

The key take-away is that even when an exact CD term is complicated, approximations guided by the variational principles can provide workable shortcuts to adiabaticity.

4.1 Vector and Star Products

We introduce a vector notation [8] which can simplify the matrix calculations.

Each element X of an algebra $\mathfrak{g} \subset \mathfrak{gl}(n)$ can be expanded in its basis $\lambda_1, \ldots, \lambda_N$ as $X = x_1\lambda_1 + \cdots + x_N\lambda_N$ and represented as a vector $\vec{x} = (x_1, \ldots, x_N)^T$.

Although this section is valid in the general case, in the rest of the thesis, we will be particularly concerned with the $\mathfrak{su}(2)$ algebra whose basis will be the Pauli matrices $\sigma_1, \sigma_2, \sigma_3$ and the $\mathfrak{su}(3)$ algebra where the basis the Gell-Mann matrices from Eq. (6.1).

The algebra can be characterized by its **structure constants** f and d which are defined respectively by the commutation and anticommutation relations

$$\begin{aligned} [\lambda_a, \lambda_b] &= 2if_{abc}\lambda_c, \\ \{\lambda_a, \lambda_b\} &= \frac{4}{N}\delta_{ab}\mathbf{1} + 2d_{abc}\lambda_c. \end{aligned} \tag{4.1}$$

To calculate the structure constants explicitly, we can use that $\mathrm{Tr}(\lambda_c^2) = 2$ to get

$$\begin{aligned} f_{abc} &= -\frac{i}{4}\mathrm{Tr}([\lambda_a, \lambda_b]\lambda_c), \\ d_{abc} &= \frac{1}{4}\mathrm{Tr}(\{\lambda_a, \lambda_b\}\lambda_c). \end{aligned} \tag{4.2}$$

By defining a dot, star and cross products between vectors as

$$\begin{aligned} \vec{x} \cdot \vec{y} &= x_c y_c, \\ (\vec{x} \star \vec{y})_a &= d_{abc} x_b y_c, \\ (\vec{x} \times \vec{y})_a &= f_{abc} x_b y_c, \end{aligned} \tag{4.3}$$

we can now perform all matrix operations as vector operations:

$$\begin{aligned} [x, y] &= x_a y_b [\lambda_a, \lambda_b] = 2i(\vec{x} \times \vec{y}) \cdot \vec{\lambda}, \\ \{x, y\} &= x_a y_b \{\lambda_a, \lambda_b\} = \frac{4}{N}\vec{x} \cdot \vec{y}\, \mathbf{1} + 2(\vec{x} \star \vec{y}) \cdot \vec{\lambda}, \end{aligned} \tag{4.4}$$

where $\vec{\lambda} = (\lambda_1, \lambda_2, ...\lambda_n)$. The addition of matrices corresponds to vector addition, and the matrix multiplication can be represented as $XY = 1/2(\{X, Y\} + [X, Y])$.

In the $SU(2)$ case, the anticommutator structure constants are zero, which simplifies the algebra:

$$\{\sigma_a, \sigma_b\} = 2\delta_{ab} \Rightarrow d_{abc} = 0 \Rightarrow \{X, Y\} = 2\vec{x} \cdot \vec{y}\mathbf{1}. \tag{4.5}$$

The vector notation will be particularly useful in Sections 5.1 and 6.4, where we use it to find expressions for the Kato gauge potentials.

4.2 Approximate Gauge Potentials

In most quantum mechanical problems, finding the spectrum of the Hamiltonian is analytically impossible, and even computationally difficult. Approximate methods allow us to find the gauge potential without knowing the explicit unitary transformation that would diagonalize the Hamiltonian.

4.2.1 Least Action Principle

We can use the idea from Eq. (2.13) to derive an expression for the commutator $[\mathcal{A}, H]$. This time, after differentiating Eq. (2.11), we substitute the derivatives of ψ_n, ψ_m with Eq. (2.32).

The derivative of $\langle\psi_m|H(t)|n\rangle$ gives

$$\begin{aligned} \partial_\lambda \langle\psi_m|H|\psi_n\rangle &= \langle\partial_\lambda\psi_m|H|n\rangle + \langle\psi_m|H|\partial_\lambda\psi_n\rangle + \langle\psi_m|\dot{H}|n\rangle \\ &= \langle\psi_m|i\mathcal{A}_\lambda H|n\rangle + \langle\psi_m| - iH\mathcal{A}_\lambda|n\rangle + \langle\psi_m|\dot{H}|n\rangle \\ &= \langle\psi_m|i[\mathcal{A}_\lambda, H] + \dot{H}|\psi_n\rangle \end{aligned} \tag{4.6}$$

On the other hand,

$$\langle\psi_m|H|\psi_n\rangle = \delta_{mn}E_n \Rightarrow \partial_\lambda\langle\psi_m|H|\psi_n\rangle = \delta_{mn}\partial_\lambda E_n. \tag{4.7}$$

We can combine all components of (4.6) to a matrix equation:

$$M_\lambda = i[\mathcal{A}_\lambda, H] + \partial_\lambda H, \tag{4.8}$$

where

$$M_\lambda = \sum_n \partial_\lambda E_n \left|\psi_n\right\rangle \left\langle\psi_n\right|. \tag{4.9}$$

The diagonal elements are generalized forces corresponding to different eigenstates.

Solving the equation

$$G(\mathcal{X}) = \partial_\lambda H + i[\mathcal{X}, H] = -M_\lambda \tag{4.10}$$

for $\mathcal{X}$ would give us $\mathcal{X} = \mathcal{A}_\lambda$. However, we can also use this equation to find $\mathcal{A}_\lambda$ variationally [9]. To do so, we minimize the Frobenius norm $||G(\mathcal{X})+M||^2 = \mathrm{Tr}(G(\mathcal{X})+M_\lambda)^2$.

$$\mathrm{Tr}[(G + M_\lambda)^2] = \mathrm{Tr}(G^2) + \mathrm{Tr}(M_\lambda^2) + 2\mathrm{Tr}(M_\lambda G), \tag{4.11}$$

$$\mathrm{Tr}(M_\lambda G) = \mathrm{Tr}(M_\lambda \partial H) + i\mathrm{Tr}(M_\lambda[\mathcal{X}, H]) = -\mathrm{Tr}(M_\lambda^2), \tag{4.12}$$

$$\mathrm{Tr}[(G + M_\lambda)^2] = \mathrm{Tr}[G^2] - \mathrm{Tr}[M_\lambda^2]. \tag{4.13}$$

Therefore we only need to minimize the "action"

$$S = \mathrm{Tr}[G^2]. \tag{4.14}$$

We can indeed call this function action, because its minimization leads to the the equations of motion:

$$\left.\frac{\delta S}{\delta \mathcal{X}}\right|_{\mathcal{X}=\mathcal{A}_\lambda} = 0 \;\Rightarrow\; [H, \partial_\lambda H + i\,[\mathcal{A}_\lambda, H]] = 0. \tag{4.15}$$

4.2.2 Least Action Principle for Floquet Systems

Suppose we have a Floquet system. We know the Hamiltonian of the system H and we want to find the Floquet Hamiltonian H_F and the micromotion operator P. We remind that during our analysis of Floquet systems, we always look at gauge potentials with respect to time, so the parameter λ from Sec. 4.2.1 is now $\lambda = t$.

This time, P is generated by the Floquet gauge potential $\mathcal{A}_F$. We cannot use (4.10) to find it variationally, because $\mathcal{A}_F$ is the gauge potential to the unknown H_F:

$$G(\mathcal{A}_F) = \partial_t H_F + i[\mathcal{X}, H_F] = -M = 0. \tag{4.16}$$

Here, $M = 0$, because H_F has constant eigenenergies. To rule out the unknown H_F from the above equation, we substitute $H(t) = H_F[t] + \mathcal{A}_F$:

$$\begin{aligned} G(\mathcal{A}_F) &= \partial_t H - \partial_t \mathcal{A}_F + i[\mathcal{A}_F, H - \mathcal{A}_F] \\ &= -i[H, \mathcal{A}_F] + \partial_t H - \partial_t \mathcal{A}_F, \end{aligned} \tag{4.17}$$

This is a known result, for example see [2].

4.2.3 Variational Principle for Floquet Systems

We can use a variational ansatz $\mathcal{X}(\alpha)$ to calculate $S(G(\mathcal{X}))$. The optimal α^* will satisfy the equation

$$\left.\frac{\partial S}{\partial \alpha}\right|_{\alpha^*} = 0. \tag{4.18}$$

To find a periodic gauge potential, we can use a periodic variational ansatz. The most general periodic operator with angular frequency ω can be decomposed with Fourier series, taking the form

$$X = \sum_{m=1}^{N_0} \sum_{l=-\infty}^{\infty} x_{lm} e^{il\omega t} \mathcal{O}_m, \tag{4.19}$$

where x_{lm} are coefficients, while $e^{il\omega t}$ and $\mathcal{O}_n$ are the bases of the decomposition. The Fourier basis's l-th component $e^{il\omega t}$ is the l-th harmonic. The operator basis $\mathcal{O}_m$ depends on the dimensionality of the system. For a two level system, it consists of $\mathbf{1}$ and the Pauli matrices $(\sigma_x, \sigma_y, \sigma_z)$. For a three-level system, it is $(\mathbf{1}, \lambda_i)$, where λ_i are the Gell-Mann matrices.

Computing G requires computing derivatives and commutators in the operator-Fourier basis.

Derivatives can be calculated as

$$(\partial_t X)_{lm} = i\omega l x_{lm}. \tag{4.20}$$

The commutator of matrices A and B with coefficients a_{lm} and b_{lm} is given by

$$[A, B]_{lm} = \sum_j \sum_k 2i f_{jkm} \sum_n a_{nj} b_{l-n,k}, \tag{4.21}$$

where f are the structure constants for the operator basis.

The anticommutator for $m \neq 0$ has the form

$$\{A, B\}_{lm} = \sum_j \sum_k 2 d_{jkm} \sum_n a_{nj} b_{l-n,k} + 2 \sum_n (a_{nm} b_{l-n,0} + a_{n0} b_{l-n,m}) \tag{4.22}$$

and for $m = 0$,

$$\{A, B\}_{l0} = \frac{4}{N} \sum_j \sum_n a_{nj} b_{l-n,j} + 2 \sum_n a_{n0} b_{l-n,0}. \tag{4.23}$$

Periodic kick operator

The Floquet theorem requires the micromotion operator, generated by $\mathcal{A}_F$, to be periodic, $P(t+T) = P(t)$. We will use Fourier-type ansatz for the "kick operator" $K(t)$, corresponding to the matrix log of the periodic micromotion operator:

$$P(t) = e^{iK(t)}. \tag{4.24}$$

This guarantees periodic micromotion. We should note that taking the matrix log can cause discontinuity of K, e.g.

$$P(t) = \exp\left(i\frac{2k\pi t}{T}\vec{n}\cdot\vec{\lambda}\right) \tag{4.25}$$

is periodic for any $k \in \mathbb{Z}$, $|\vec{n}| = 1$. When searching for K using finite harmonics, we cannot find discontinuous or non-periodic kick operators which would exponentiate to P. However, such *whole number turns* can be transferred from the micromotion operator to the Floquet Hamiltonian:

$$U = P(t)e^{-itH_F} = P'(t)e^{-itH'_F}. \tag{4.26}$$

Calculating the gradients

We begin with the ansatz

$$K = \sum_{m=1}^{N_0}\sum_{l=N}^{N} k_{ml}e^{il\omega t}\mathcal{O}_m. \tag{4.27}$$

The associated gauge potential can be computed as

$$\begin{aligned}\mathcal{A}_F &= i\dot{P}P^\dagger = i\frac{d}{dt}e^{iK(t)}e^{-iK(t)} \\ &= i\left(i\dot{K}(t) - \frac{1}{2!}[K,\dot{K}] - \frac{i}{3!}[K,[K,\dot{K}]] + ...\right).\end{aligned} \tag{4.28}$$

To simplify such nested commutator expressions, we use the notation

$$\mathrm{ad}_X Y = [X,Y], \quad \mathrm{ad}_X^n Y = [X,\mathrm{ad}_X^{n-1}Y], \tag{4.29}$$

giving

$$\mathcal{A} = -\sum_{n=0}^{\infty}\frac{i^n}{(n+1)!}\mathrm{ad}_K^n\dot{K}. \tag{4.30}$$

Next, G has the form

$$G(\mathcal{A}_F) = i[H,\mathcal{A}_F] - \partial_t H + \partial_t\mathcal{A}_F = 0 \tag{4.31}$$

and we try to minimize the cost function

$$S = \mathrm{Tr}G^2. \tag{4.32}$$

To find the minimum of the cost function with respect to the variational parameters k_{nl} using gradient descent, we need to compute its derivative.

$$\begin{aligned}\partial_{k_{nl}}S &= \partial_{k_{nl}}\mathrm{Tr}G^2 = 2\mathrm{Tr}G\partial_{k_{nl}}G \\ &= 2\mathrm{Tr}G\left(i[H,\partial_{k_{nl}}\mathcal{A}] + \partial_{k_{nl}}\partial_t\mathcal{A}\right).\end{aligned} \tag{4.33}$$

To compute $\partial_{k_{nl}}\mathcal{A}$, we first need to figure out the derivative of a nested commutator:

$$\begin{aligned}\partial_\lambda \mathrm{ad}_X^n Y &= [\partial_\lambda X, \mathrm{ad}_X^{n-1} Y] + [X, \partial_\lambda \mathrm{ad}_X^{n-1} Y] \\ &= \sum_{m=0}^{n-1} \mathrm{ad}_X^m [\partial_\lambda X, \mathrm{ad}_X^{n-1-m} Y] + \mathrm{ad}_X^n \partial_\lambda Y.\end{aligned} \tag{4.34}$$

With this rule for differentiating nested commutators, the derivative of $\mathcal{A}$ becomes

$$\partial_{k_{nl}} \mathcal{A} = -\sum_{n=0}^{\infty} \frac{i^n}{(n+1)!} \left(\sum_{m=0}^{n-1} \mathrm{ad}_K^m [\partial_{k_{nl}} K, \mathrm{ad}_K^{n-1-m} \dot{K}] + \mathrm{ad}_K^n \partial_{k_{nl}} \dot{K} \right). \tag{4.35}$$

Differentiating the kick operator itself yields

$$\partial_{k_{nl}} K = e_{nl}, \quad \partial_{k_{nl}} \dot{K} = -i\omega l e_{nl}, \tag{4.36}$$

where e_{nl} is a matrix whose only non-zero element is $(e_{nl})_{nl} = 1$is zero everywhere except the n, l-th element, which is 1. The final expression for the derivatives of $\mathcal{A}$,

$$\partial_{k_{ml}} \mathcal{A} = -\sum_{n=0}^{\infty} \frac{i^n}{(n+1)!} \left(\sum_{k=0}^{n-1} \mathrm{ad}_K^k [e_{ml}, \mathrm{ad}_K^{n-1-k} \dot{K}] - i\omega l \mathrm{ad}_K^n e_{nl} \right), \tag{4.37}$$

can be plugged in (4.33) to compute the derivative of S. Then, finding the minimum of S can be done with gradient descent.

Modified Gradient Descent

To finalize the algorithm we use to find the gauge potentials of various systems (Sec. 5.3, 5.4, 7.1), we had to enhance the gradient descent algorithm. The problem is that calculating a single gradient using (4.33) is a computationally costly task. We had to minimize the number of calculations of the gradient, instead adding auxiliary simpler checks. The end result is a gradient descent Algorithm 1.

First, we adapt the step size η by estimating the second derivative in the direction of the descent. Then, even if the second derivative is negative, we take a step. We do not calculate any gradients until we descended away from the area with negative second derivative. Finally, after calculating a gradient, we use momentum-based gradient descent. This helps the algorithm to converge faster, because it will not get stuck oscillating along a convex direction.

Algorithm 1 Pseudocode for the modified gradient descent

initialize $K \leftarrow H$
initial step size $\eta = 3 \cdot 10^{-4}$
initial gradient $g = \nabla_K S$
for each episode **do**
    $S_0 = S(K)$, $S_1 = S(K - \eta g)$, $S_2 = S(K - 2\eta g)$ ▷ find the cost after moving along the gradient
    $\eta' = \eta(1 + (S_2 - S_0)/(4S_1 - 2S_2 - S_0))$ ▷ estimate the best step size with Newton's method
    if $S_1 > S_2$ **then** ▷ taking one step does not lower the cost
        $\eta \leftarrow \eta/2$ ▷ lower the step size
    else if $\eta' < 0$ **then** ▷ negative second derivative
        $K \leftarrow K - \eta g$
        $\eta \leftarrow 2\eta$
    else if $\eta' < \eta/2$ **then** ▷ the step size is too large
        $\eta \leftarrow \eta/2$
    else if $\eta' > 2\eta$ **then** ▷ the step size is too small
        $\eta \leftarrow \eta/2$
    else
        $K \leftarrow K - (\eta + \eta')g/2$
        $g \leftarrow 0.9g + \nabla_K S$ ▷ gradient descent with momentum
        $\eta \leftarrow \eta'$
    end if
end for

Chapter 5

Counter-Diabatic Driving for Periodically Driven Two Level Systems

In this chapter, we apply the CD driving framework to the simplest non-trivial case: two-level systems. Despite their relatively simple dynamics, these systems are interesting on their own – such systems are qubits and the spin-1/2 particles. We derive the closed-form expression for the Kato gauge potential starting from the variational principle, and a parametric form of the AGP for a generic traceless two-level Hamiltonian.

In this chapter, we also perform numerical experiments. We use the variational method to find gauge potentials for particular periodically driven 2LS. The systems are a spin-1/2 particle in magneetic field, interacting with either a circularly, or a linearly polarized field. The circular field problem is analytically solvable. We present the analytical solution and compare it with the variational gauge potential. For the linear drive, we confirm the accuracy of the variational gauge potential with another numerical method. This paves the way to Chapter 6 and 7, where we tackle the richer three-level case.

5.1 Kato Gauge Potential

We find the closed form expression of the Kato gauge potential of a two-level system with traceless Hamiltonian by taking advantage of the variational principle discussed in Sec. 4.2.3. The Hamiltonian can take the form

$$H = \vec{h} \cdot \vec{\sigma}. \tag{5.1}$$

We are looking for a gauge potential of the form

$$\mathcal{A} = \vec{a} \cdot \vec{\sigma}. \tag{5.2}$$

The Kato potential minimizes $S = \mathrm{Tr}G^2$ (see eq. (4.14)), where

$$G = \partial_\lambda H + i[\mathcal{A}, H]. \tag{5.3}$$

Using vector notation,

$$[\mathcal{A}, H] = 2i(\vec{a} \times \vec{h}) \cdot \vec{\sigma}, \tag{5.4}$$

$$\begin{aligned} G_\lambda^2 &= ((\partial_\lambda \vec{h} - 2(\vec{a} \times \vec{h})) \cdot \vec{\sigma})^2 \\ &= (\partial_\lambda \vec{h} - 2(\vec{a} \times \vec{h}))^2 \mathbf{1}, \end{aligned} \tag{5.5}$$

$$S = \mathrm{Tr}(G_\lambda^2) = 2(\partial_\lambda \vec{h} - 2(\vec{a} \times \vec{h}))^2, \tag{5.6}$$

$$\begin{aligned} \nabla_{\vec{a}} S &= 4(\partial_\lambda \vec{h} - 2(\vec{a} \times \vec{h})) \cdot (-2\nabla_{\vec{a}}(\vec{a} \times \vec{h})) \\ &= -8(\partial_\lambda \vec{h} - 2(\vec{a} \times \vec{h})) \times \vec{h} = 0. \end{aligned} \tag{5.7}$$

In order for the vector product to be zero, either $\vec{h} = 0$, or $\partial_\lambda \vec{h} - 2\vec{a} \times \vec{h}$ is parallel to $\vec{h}$. Let

$$\partial_\lambda \vec{h} - 2\vec{a} \times \vec{h} = k\vec{h}. \tag{5.8}$$

We can find k by dot multiplying the equation by $\vec{h}$ and using $(\vec{a} \times \vec{h}) \cdot \vec{h} = 0$:

$$(\partial_\lambda \vec{h}) \cdot \vec{h} = kh^2, \tag{5.9}$$

$$\vec{a} \times \vec{h} = \frac{\partial_\lambda \vec{h} h^2 - (\partial_\lambda \vec{h} \cdot \vec{h})\vec{h}}{2h^2}, \tag{5.10}$$

$$\vec{a} \times \vec{h} = \frac{(\vec{h} \times \partial_\lambda \vec{h}) \times \vec{h}}{2h^2}, \tag{5.11}$$

$$\vec{a} = \frac{\vec{h} \times \partial_\lambda \vec{h}}{2h^2}. \tag{5.12}$$

The last step technically gives $\vec{a}$ up to addition with const$\cdot\vec{h}$. However, the Kato potential must also satisfy the condition that its diagonal elements are zero in eigenbasis of H. That restricts $\vec{a}$ to Eq. (5.12).

5.2 Adiabatic Gauge Potential Parametrization

The general traceless two-level system Hamiltonian has the form

$$H(t) = \vec{h}(t) \cdot \vec{\sigma} = h(t)\vec{n}(t)\vec{\sigma}, \tag{5.13}$$

where the normal unitary vector $\vec{n}$ can be decomposed in spherical coordinates,

$$\vec{n}(t) = \begin{pmatrix} \sin\theta(t)\cos\phi(t) \\ \sin\theta(t)\sin\phi(t) \\ \cos\phi(t) \end{pmatrix}. \tag{5.14}$$

We can diagonalize the Hamiltonian by rotating with angle ϕ along the z-axis,

$$\begin{aligned} R_z^\dagger(\vec{n} \cdot \vec{\sigma})R_z &= \cos\theta\sigma_z + \sin\theta(\cos^2\phi\sigma_x - \cos\phi\sin\phi\sigma_y + \sin\phi\cos\phi\sigma_y + \sin^2\phi\sigma_x) \\ &= \cos\theta\sigma_z + \sin\theta\sigma_x, \end{aligned} \tag{5.15}$$

then rotating with angle θ along the y-axis:

$$R_y^\dagger R_z^\dagger(\vec{n} \cdot \vec{\sigma})R_z R_y = \cos^2\theta\sigma_z - \cos\theta\sin\theta\sigma_x + \sin\theta\cos\theta\sigma_x + \sin^2\theta\sigma_z = \sigma_z. \tag{5.16}$$

We calculate the gauge potential corresponding to the transformation $U = R_z R_y$:

$$\tilde{\mathcal{A}}_t = iU^\dagger \dot{U} = iU^\dagger \partial_\theta U \dot{\theta} + iU^\dagger \partial_\phi U \dot{\phi} = \dot{\theta}\tilde{\mathcal{A}}_\theta + \dot{\phi}\tilde{\mathcal{A}}_\phi, \tag{5.17}$$

$$\begin{aligned}\tilde{\mathcal{A}}_\phi &= iR_y^\dagger R_z^\dagger \partial_\phi R_z R_y \\ &= iR_y^\dagger R_z^\dagger \left(-\frac{i}{2}\right) R_z \sigma_z \\ &= \frac{1}{2} R_y^\dagger \sigma_z R_y = \frac{1}{2}(\cos\theta\sigma_z - \sin\theta\sigma_x),\end{aligned} \tag{5.18}$$

$$\begin{aligned}\mathcal{A}_\phi &= U\tilde{\mathcal{A}}_\phi U^\dagger \\ &= R_z R_y \left(\frac{1}{2} R_y^\dagger \sigma_z R_y\right) R_y^\dagger R_z^\dagger \\ &= \frac{1}{2} R_z \sigma_z R_z^\dagger = \frac{\sigma_z}{2},\end{aligned} \tag{5.19}$$

$$\tilde{\mathcal{A}}_\theta = iR_y^\dagger R_z^\dagger R_z \partial_\theta R_y = iR_y^\dagger \partial_\theta R_y = \sigma_y/2, \tag{5.20}$$

$$\mathcal{A}_\theta = \frac{1}{2} R_z R_y \sigma_y R_y^\dagger R_z^\dagger = \frac{1}{2} R_z \sigma_y R_z^\dagger = \frac{1}{2}(\cos\phi\sigma_y - \sin\phi\sigma_x). \tag{5.21}$$

We have used equations (A.3) and (A.5) about the rotation matrices from App. A.

Note that the although the operator $U = R_z R_y$ is unitary, it adds a global phase to the wave function:

$$\begin{aligned}R_z(\phi)R_y(\theta) &= e^{-i\frac{\phi}{2}\sigma_z} e^{-i\frac{\theta}{2}\sigma_y} \\ &= \left(\cos\left(\frac{\phi}{2}\right)\mathbf{1} - i\sin\left(\frac{\phi}{2}\right)\sigma_z\right)\left(\cos\left(\frac{\theta}{2}\right)\mathbf{1} - i\sin\left(\frac{\theta}{2}\right)\sigma_y\right) \\ &= \begin{pmatrix}\cos(\phi/2) - i\sin(\phi/2) & 0 \\ 0 & \cos(\phi/2) + i\sin(\phi/2)\end{pmatrix}\begin{pmatrix}\cos(\theta/2) & -\sin(\theta/2) \\ \sin(\theta/2) & \cos(\theta/2)\end{pmatrix} \\ &= e^{-i\phi/2}\begin{pmatrix}\cos(\theta/2) & -\sin(\theta/2) \\ e^{i\phi}\sin(\theta/2) & e^{i\phi}\cos(\theta/2)\end{pmatrix}.\end{aligned} \tag{5.22}$$

We note that the eigenstates of the general Hamiltonian (5.13) are defined up to a global phase:

$$|\psi_{\text{instantaneous}}(t)\rangle = e^{i\alpha}\begin{pmatrix}\cos\frac{\theta}{2} \\ e^{i\phi}\sin\frac{\theta}{2}.\end{pmatrix} \tag{5.23}$$

In the current convention $U = R_z R_y$, the eigenstates accumulate a global phase

$$\alpha(t) = e^{-i\frac{\phi}{2}}. \tag{5.24}$$

To remove the global phase, we can use the transformation matrix

$$U' = \begin{pmatrix}\cos(\theta/2) & -\sin(\theta/2) \\ e^{i\phi}\sin(\theta/2) & e^{i\phi}\cos(\theta/2)\end{pmatrix}. \tag{5.25}$$

Using U' instead of U affects the ϕ-component of the gauge potential – we denote the new AGP $\mathcal{A}'_\phi$ and the new AGP in the rotating frame is respectively $\tilde{\mathcal{A}}'_\phi$:

$$\begin{aligned}\tilde{\mathcal{A}}'_\phi &= iU^\dagger e^{-i\phi/2}\partial_\phi(e^{i\phi/2}U) \\ &= \tilde{\mathcal{A}}_\phi + iU^\dagger e^{-i\phi/2}\frac{i}{2}e^{i\phi/2}U \\ &= \frac{1}{2}(\cos\theta\sigma_z - \sin\theta\sigma_x) - \frac{\mathbf{1}}{2} \qquad (5.26)\\ \mathcal{A}'_\phi &= \frac{\sigma_z}{2} - \frac{\mathbf{1}}{2}. \qquad (5.27)\end{aligned}$$

5.3 Example: Circular Drive

Now, we turn to turn to some particular two-level systems, where we test the variational approach from Sec. 4.2.3. We begin with a theoretically solvable quantum mechanical problem.

Problem Setup

Consider the two level system

$$H(t) = \frac{\Delta}{2}\sigma_z + \frac{g}{2}\left(\cos\omega t\sigma_x + \sin\omega t\sigma_y\right), \qquad (5.28)$$

which has energy gap Δ and is interacting with a circularly polarized field of strength g. This is one of the few systems that can be solved exactly analytically.

Theoretical Solution

The Hamiltonian rotates with angular frequency ω around the σ_z-axis. To make it static, we rotate (A.1) the reference frame along the z axis:

$$R_z(\omega(t-t_0)) = e^{-i\omega/2(t-t_0)\sigma_z}, \qquad (5.29)$$

turning the Hamiltonian to

$$\begin{aligned}H_{\text{rot}}[t_0] &= R_z^\dagger H R_z - iR_z^\dagger\partial_t R_z \\ &= \frac{\Delta}{2}\sigma_z + \frac{g}{2}\left(\cos(\omega t_0)\sigma_x + \sin(\omega t_0)\sigma_y\right) - \frac{\omega}{2}\sigma_z \qquad (5.30)\\ &= \frac{\varepsilon}{2}\hat{n}(\omega t_0,\beta)\cdot\vec{\sigma},\end{aligned}$$

where

$$\varepsilon = \sqrt{(\Delta-\omega)^2 + g^2}, \qquad (5.31)$$

$$\hat{n}(\theta,\phi) = (\sin\theta\cos\phi, \sin\theta\sin\phi, \cos\theta) \qquad (5.32)$$

and

$$\sin\beta = \frac{g}{\varepsilon}. \qquad (5.33)$$

This Hamiltonian explodes at $\omega \to \infty$. To make a suitable Floquet Hamiltonian, we can represent the evolution as

$$\begin{aligned} U(t;t_0) &= R_z(\omega(t-t_0))e^{-(t-t_0)H_{rot}[t_0]}R_z^\dagger(0) \\ &= R_z(\omega(t-t_0))(t,t_0)e^{-i\omega/2(t-t_0)\hat{n}(\omega t;\hat{\beta})\cdot\vec{\sigma}}e^{-i(t-t_0)(1-\frac{\omega}{\varepsilon})H_{rot}[t_0]}, \end{aligned} \tag{5.34}$$

giving us a micromotion operator

$$P_{FM} = e^{-i\omega/2(t-t_0)\sigma_z}e^{-i\omega/2(t-t_0)\hat{n}(\omega t;\hat{\beta})\cdot\vec{\sigma}} \tag{5.35}$$

and a Floquet Hamiltonian

$$\begin{aligned} H_{FM}[t_0] &= (1-\frac{\omega}{\varepsilon})H_{rot}[t_0] = \\ &= \frac{1}{2}(\varepsilon-\omega)\hat{n}(\omega t_0;\hat{\beta})\cdot\vec{\sigma}, \end{aligned} \tag{5.36}$$

which corresponds to the Floquet-Magnus expansion at $\omega \to \infty$.

$$P_{FM}(t;t_0) = P_{rot}(t,t_0)e^{-i\omega/2(t-t_0)\hat{n}(\omega t;\hat{\beta})\cdot\vec{s}} \tag{5.37}$$

We can calculate the associated Floquet gauge potential:

$$\begin{aligned} \mathcal{A}_{FM}^U(t;t_0) &= (i\partial_t P_{FM}(t;t_0))P_{FM}^\dagger(t;t_0) \\ &= \frac{\omega}{2}\sigma_z + \frac{\omega}{2}\hat{n}(\omega t;\hat{\beta})\cdot\vec{\sigma}. \end{aligned} \tag{5.38}$$

Variational approach

We can find the Floquet Hamiltonan using the variational principle from Sec. 4.2.3.

We are looking for a kick operator K, such that $P = e^{iK}$ is the micromotion operator. K is parametrized as

$$K = \sum_{m=1}^{N_0}\sum_{l=N}^{N} k_{ml}e^{il\omega t}\sigma_m, \tag{5.39}$$

where k_{ml} are the variational coefficients. We make some initial guess for the kick operator K. Then, we minimize the action (4.14) using gradient descent, as discussed in Sec. 4.2. After finding the optimal kick operator, we use Eq. (4.28) to find its associated Floquet gauge potential. Then, the Floquet Hamiltonian is simply

$$H_F[t] = H(t) - \mathcal{A}_F(t). \tag{5.40}$$

The variationally-obtained Floquet Hamiltonan is plotted with a dashed line on Fig. 5.1 a). It matches with the theoretical solution (5.36), plotted with a solid line. As we can see, the variational method provides a very high-fidelity AGP.

5.4 Example: Linear Drive

We have tested the variational Floquet AGP in a system with unknown theoretical solution.

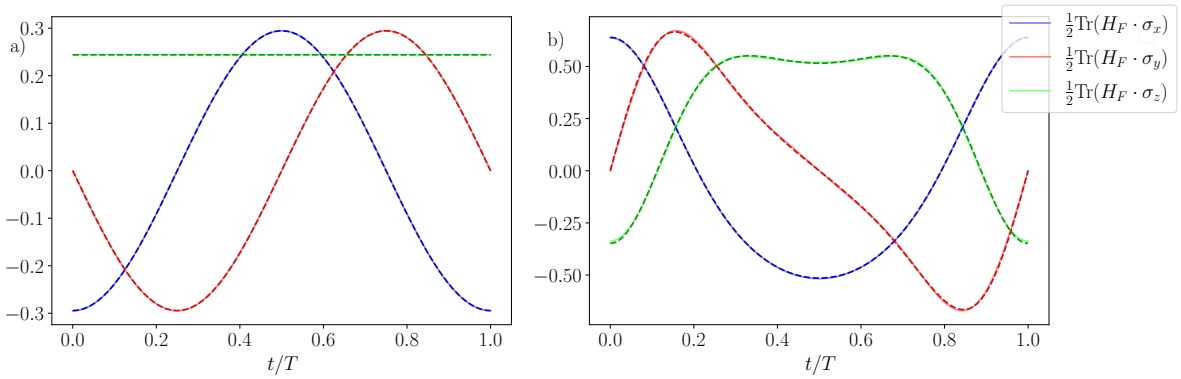

Figure 5.1: Components of the Floquet Hamiltonian in the Pauli basis for: a) circularly driven system in Sec. 5.3. Found with variational method (solid line) vs theoretical solution (dashed line), $g/\Delta = 0.5$, $\omega/\Delta = \sqrt{2}$; b) linearly driven system in Sec. 5.4. Found with variational method (solid line) vs numerical integration (dashed line), $\omega/\Delta = 1$, $g/\Delta = 0.5$. Number of harmonics used: 3. In both cases, the variational method obtains a high-fidelity counter-diabatic drive.

Consider the linearly driven two level system

$$H(t) = \frac{\Delta}{2}\sigma_z + \frac{g}{2}\left(1 + 2\cos\omega t\right)\sigma_x, \tag{5.41}$$

where Δ is the energy gap and g is the strength of interaction with the linearly polarized field.

We obtain the Floquet Hamiltonian using the variation principle by exactly the same method as in Sec. 5.3, plotted as a dashed line in Fig. 5.1 b).

Apart of the fact that the variational algorithm converged ($S \sim 10^{-8}$), we can verify the obtained Floquet Hamiltonian by finding it numerically in a more direct way.

First, we numerically integrate Schrodinger's equation

$$i\partial_t \left|\psi\right\rangle = H \left|\psi\right\rangle \tag{5.42}$$

for one period $T = 2\pi/\omega$, starting at $|0\rangle$ and $|1\rangle$. This gives us the components of the Floquet unitary U_F. Then, the Floquet Hamiltonian satisfies

$$e^{-iTH_F} = U_F. \tag{5.43}$$

To find H_F, we take the matrix logarithm of U_F numerically.

However, the matrix logarithm is not uniquely defined. The Floquet Hamiltonian, respectively, has undefined energy levels. Taking the principal logarithm returns a Floquet Hamiltonain H_{F0} with energy levels inside the *Floquet zone*. Then, any Hamiltonian in the form

$$H_F = H_{F0} + \omega R \mathrm{diag}(k_1, ...k_n) R^\dagger, \tag{5.44}$$

where R is a unitary matrix diagonalizing H_{F0}, $k_1, ...k_n \in \mathbb{Z}$, $n = \mathrm{dim}H$, $\sum k_i = 0$ is a valid Floquet Hamiltonian:

$$U_F = e^{-iTH_{F0}} = e^{-iTH_{F0}} e^{-i2\pi R \mathrm{diag}(k_1,...k_n)R^\dagger} = e^{-iTH_F} \tag{5.45}$$

In our case, $n = 2$, it turns out that the variational solution matches the Hamiltonian, obtained by adding $k_1 = 1$ and $k_2 = -1$ to the principal matrix logarithm. The resulting Floquet Hamiltonian is shown with a solid line in Fig. 5.1 b).

Chapter 6

Three Level Systems

In this chapter, we explore part of the theory behind three level systems. Such systems arise naturally in many fields of quantum physics. One of the most common examples of such system is the lambda system that we address in Sec. 7.1.

To describe the state of a three level system, we need three dimensional kets. The evolution of such systems is given by a 3×3 unitary matrix, and as the global phase of the quantum state is irrelevant, the only physically meaningful evolution operators are from the $SU(3)$ group – unitary, and with determinant 1.

The Hamiltonians governing the evolution of a general three level system are 3×3 Hermitian matrices. In terms of the Hamiltonian, the non-physical global phase is acquired by evolving with a constant Hamiltonian – adding a constant energy to the whole system. If we discard it, we are left with *traceless* Hamiltonians. They are elements of the $\mathfrak{su}(3)$ **algebra** and generate the $SU(3)$ group of evolution operators.

To study the gauge potentials in three level systems, we need to understrand the structure of $SU(3)$.

6.1 Structure of the SU(3) Group

The most commonly used basis of the $\mathfrak{su}(3)$ algebra is the Gell-Mann matrices

$$\begin{aligned}
\lambda_1 &= \begin{pmatrix} 0 & 1 & 0 \\ 1 & 0 & 0 \\ 0 & 0 & 0 \end{pmatrix} & \lambda_2 &= \begin{pmatrix} 0 & -i & 0 \\ i & 0 & 0 \\ 0 & 0 & 0 \end{pmatrix} & \lambda_3 &= \begin{pmatrix} 1 & 0 & 0 \\ 0 & -1 & 0 \\ 0 & 0 & 0 \end{pmatrix} \\
\lambda_4 &= \begin{pmatrix} 0 & 0 & 1 \\ 0 & 0 & 0 \\ 1 & 0 & 0 \end{pmatrix} & \lambda_5 &= \begin{pmatrix} 0 & 0 & -i \\ 0 & 0 & 0 \\ i & 0 & 0 \end{pmatrix} \\
\lambda_6 &= \begin{pmatrix} 0 & 0 & 0 \\ 0 & 0 & 1 \\ 0 & 1 & 0 \end{pmatrix} & \lambda_7 &= \begin{pmatrix} 0 & 0 & 0 \\ 0 & 0 & -i \\ 0 & i & 0 \end{pmatrix} \\
\lambda_8 &= \tfrac{1}{\sqrt{3}} \begin{pmatrix} 1 & 0 & 0 \\ 0 & 1 & 0 \\ 0 & 0 & -2 \end{pmatrix}
\end{aligned} \tag{6.1}$$

Subgroup	Generators	Elements of the subgroup
$SU(2)$	$\lambda_1,\ \lambda_2,\ \lambda_3$	$\left(\begin{array}{cc\|c} & & 0 \\ & u & 0 \\ \hline 0 & 0 & 1 \end{array}\right),\ u \in SU(2)$
$SU(2)$	$\lambda_4,\ \lambda_5,\ H_1$	$\left(\begin{array}{c\|c\|c} & 0 & \\ \hline 0 & 1 & 0 \\ \hline & 0 & u \end{array}\right),\ u \in SU(2)$
$SU(2)$	$\lambda_6,\ \lambda_7,\ H_2$	$\left(\begin{array}{c\|cc} 1 & 0 & 0 \\ \hline 0 & u & \\ 0 & & \end{array}\right),\ u \in SU(2)$
$U(2)$	$\lambda_1,\ \lambda_2,\ \lambda_3,\ \lambda_8$	$\left(\begin{array}{cc\|c} & & 0 \\ & u & 0 \\ \hline 0 & 0 & (\det u)^{-1} \end{array}\right),\ u \in U(2)$
$SO(3)$	$\lambda_2, \lambda_5, \lambda_7$	$X(\alpha)Y(\beta)Z(\gamma)$ [1]
$U(1)$	H_1	$\begin{pmatrix} e^{i\theta_1} & 0 & 0 \\ 0 & 1 & 0 \\ 0 & 0 & e^{-i\theta_1} \end{pmatrix}$
$U(1)\times U(1)$	$H_1,\ H_2$	$\begin{pmatrix} e^{i\theta_1} & 0 & 0 \\ 0 & e^{i\theta_2} & 0 \\ 0 & 0 & e^{-i\theta_1-i\theta_2} \end{pmatrix}$

Table 6.1: A non-exhaustive list of $SU(3)$ subgroups and their generators and parameterizations. Generators include the Gell-Mann matrices (6.1) and H_1, H_2 from (6.2).

One can recognize that $\lambda_1, \lambda_2, \lambda_3$ generate a $SU(2)$ subgroup of $SU(3)$ – their upper 2×2 blocks are exactly the Pauli matrices $\sigma_1, \sigma_2, \sigma_3$. We can find infinitely many $SU(2)$ subgroups by rotating this set with arbitrary $SU(3)$ transformations. In particular, using the linear combinations

$$\begin{aligned} H_1 &= \frac{\sqrt{3}}{2}\lambda_8 + \frac{1}{2}\lambda_3 = \begin{pmatrix} 1 & 0 & 0 \\ 0 & 0 & 0 \\ 0 & 0 & -1 \end{pmatrix}, \\ H_2 &= \frac{\sqrt{3}}{2}\lambda_8 - \frac{1}{2}\lambda_3 = \begin{pmatrix} 0 & 0 & 0 \\ 0 & 1 & 0 \\ 0 & 0 & -1 \end{pmatrix}, \end{aligned} \tag{6.2}$$

we get alternative $SU(2)$ subgroups listed in Table 6.1. The $SO(3)$ subgroup can be generated by λ_2, λ_5 and λ_7.

The $U(2)$ and $U(1)\times U(1)$ subgroups and its respective coset spaces $SU(3)/U(2)$ and $SU(3)/U(1)\times U(1)$ are of special interest to us. In Sec. 6.1.1, we will see that the orbits of a Hamiltonian (6.22) span one of the coset spaces.

The $U(1)\times U(1)$ group is generated by H_1 and H_2. We can see that

$$e^{i\theta_1 H_1} e^{i\theta_2 H_2} = \begin{pmatrix} e^{i\theta_1} & 0 & 0 \\ 0 & e^{i\theta_2} & 0 \\ 0 & 0 & e^{-i\theta_1-i\theta_2} \end{pmatrix}, \tag{6.3}$$

[1] The $SO(3)$ rotations are $X = \begin{pmatrix} \cos\alpha & \sin\alpha & 0 \\ -\sin\alpha & \cos\alpha & 0 \\ 0 & 0 & 1 \end{pmatrix}$, $Y = \begin{pmatrix} \cos\beta & 0 & \sin\beta \\ 0 & 1 & 0 \\ -\sin\beta & 0 & \cos\beta \end{pmatrix}$, $Z = \begin{pmatrix} 1 & 0 & 0 \\ 0 & \cos\gamma & \sin\gamma \\ 0 & -\sin\gamma & \cos\gamma \end{pmatrix}$.

which gives us a parametrization of $U(1) \times U(1)$. Note that H_1 and H_2 are linear combinations of λ_3 and λ_8. This means that λ_3 and λ_8 also serve as generators of the same subgroup.

To construct the $U(2)$ subgroup, we use the fact that the 2×2 matrices $u \in U(2)$ are generated by $\sigma_1, \sigma_2, \sigma_3, \mathbf{1}$. Suppose

$$u = e^{i\theta_0 \mathbf{1}} e^{i\theta_1 \sigma_1} e^{i\theta_2 \sigma_2} e^{i\theta_3 \sigma_3}. \tag{6.4}$$

Since $\det(e^{i\theta_i \sigma_i}) = 1$, the determinant of u is

$$\det u = e^{2i\theta_0}. \tag{6.5}$$

In $SU(3)$, $\lambda_1, \lambda_2, \lambda_3$ contain $\sigma_1, \sigma_2, \sigma_3$ respectively in their upper 2×2 block. If we add λ_8, whose upper 2×2 block is proportional to the identity matrix, we get

$$e^{i\theta_0 \sqrt{3}\lambda_8} e^{i\theta_1 \lambda_1} e^{i\theta_2 \lambda_2} e^{i\theta_3 \lambda_3} = \begin{pmatrix} u & & 0 \\ & & 0 \\ 0 & 0 & e^{-2i\theta_0} \end{pmatrix} = \begin{pmatrix} u & & 0 \\ & & 0 \\ 0 & 0 & (\det u)^{-1} \end{pmatrix}. \tag{6.6}$$

By construction, these matrices are in $SU(3)$. Also, there is a direct correspondence between matrices of this form and matrices $u \in U(2)$, satisfying the same group relations. Therefore, these matrices, generated by $\lambda_1, \lambda_2, \lambda_3, \lambda_8$, are indeed a valid representation of $U(2) \subset SU(3)$.

Cartan decomposition

To navigate in the $SU(3)$ group, we would benefit from a complete parametrization of its elements. This can be done by a Cartan decomposition [10]. The subalgebra $\mathfrak{k} = \{\lambda_1, \lambda_2, \lambda_3, \lambda_8\}$ and its orthogonal complement $\mathfrak{p} = \{\lambda_4, \lambda_5, \lambda_6, \lambda_7\}$ constitute a Cartan pair:

$$\begin{aligned} [k_1, k_2] &\in \mathfrak{k} \quad \forall k_1, k_2 \in \mathfrak{k}, \\ [p_1, p_2] &\in \mathfrak{k} \quad \forall p_1, p_2 \in \mathfrak{p}, \\ [k, p] &\in \mathfrak{p} \quad \forall k \in \mathfrak{k}, p \in \mathfrak{p}. \end{aligned} \tag{6.7}$$

This allows the decomposition

$$SU(3) = KAK, \tag{6.8}$$

where K is the $U(2)$ subgroup $\exp(\mathfrak{k})$ and $A = \exp(\mathfrak{a})$, where $\mathfrak{a}$ is the maximal Abelian subalgebra of $\mathfrak{p}$. The algebra $\mathfrak{a}$ is one dimensional and we can chose $\mathfrak{a}$ to have a basis – one element of $\mathfrak{p}$ we want, for example λ_5:

$$A = \{e^{i\lambda_5 \theta} : \theta \in [0, 2\pi)\}. \tag{6.9}$$

The subgroup K can itself be decomposed as

$$K = \{e^{i\lambda_3 \alpha} e^{i\lambda_2 \beta} e^{i\lambda_3 \gamma} e^{i\lambda_8 \phi} : \alpha, \beta, \gamma, \phi \in [0, 2\pi)\}, \tag{6.10}$$

which is the Euler angle decomposition of $SU(2)$ plus a rotation with respect to λ_8, which commutates with the whole $SU(2)$ subgroup. As the $SU(3)$ group is 8-dimensional, one of the λ_8-rotations is redundant. This leaves us with the following parametrization of $SU(3)$:

$$U(\alpha, \beta, \gamma, \theta, a, b, c, \phi) = e^{i\lambda_3 \alpha} e^{i\lambda_2 \beta} e^{i\lambda_3 \gamma} e^{i\lambda_5 \theta} e^{i\lambda_3 a} e^{i\lambda_2 b} e^{i\lambda_3 c} e^{i\lambda_8 \phi}. \tag{6.11}$$

Coset spaces

Starting with (6.11), we can parametrize coset spaces by removing the respective subgroups.

In particular, to get the coset space $\mathscr{I} = SU(3)/U(1) \times U(1)$, we need to remove a $U(1) \times U(1)$ subgroup (6.3). If we parametrize the subgroup as $e^{i\lambda_3 c} e^{i\lambda_8 \phi}$, the remaining coset space takes the form

$$U_{\mathscr{I}} = e^{i\lambda_3 \alpha} e^{i\lambda_2 \beta} e^{i\lambda_3 \gamma} e^{i\lambda_5 \theta} e^{i\lambda_3 a} e^{i\lambda_2 b}. \tag{6.12}$$

We are also interested in the coset space $\mathscr{R} = SU(3)/U(2)$. Removing as $U(2)$ subgroup (6.10) leaves us with

$$U_{\mathscr{R}} = e^{i\lambda_3 \alpha} e^{i\lambda_2 \beta} e^{i\lambda_3 \gamma} e^{i\lambda_5 \theta}. \tag{6.13}$$

Casimir invariants

An important characteristic of the $\mathfrak{su}(3)$ algebra is its Casimir invariants, which provide us with conserved quantities.

All semisimple Lie algebras [11] – including all subalgebras of $\mathfrak{sl}(n)$ have a quadratic Casimir. In the case of $\mathfrak{su}(3)$, the quantity

$$C_2 = \sum_{i=1}^{8} \lambda_i^2 \tag{6.14}$$

indeed commutes with all elements of $\mathfrak{su}(3)$. This makes the bilinear form

$$B(X, Y) = \sum_{i=1}^{8} x_i y_i, \tag{6.15}$$

invariant, where x_i and y_j are the components of X and Y in the Gell-Mann basis.

$$B(X, Y) = \frac{1}{2} \mathrm{Tr}(X, Y) = \vec{x} \cdot \vec{y}, \tag{6.16}$$

where we have used the notations from Sec. 4.1. The "dot" product indeed plays the role of a scalar product. It stays invariant under any rotation $U \in SU(3)$. If X and Y transform to

$$\tilde{X} = UXU^{-1}, \tilde{Y} = UYU^{-1}, \tag{6.17}$$

the bilinear form will have the same value:

$$B(\tilde{X}, \tilde{Y}) = B(XY). \tag{6.18}$$

In particular, any Hamiltonian H undergoing a unitary transformation has an invariant "norm" $h = \sqrt{\vec{h}^2}$.

One can also recognize the form as proportional to the invariant Killing form [12]

$$\mathcal{B}(X, Y) = \mathrm{Tr}(\mathrm{ad}(X) \circ \mathrm{ad}(Y)) = 6\mathrm{Tr}(XY). \tag{6.19}$$

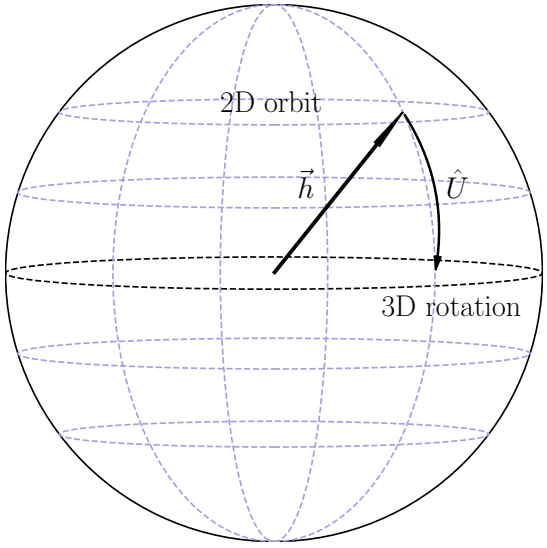

Figure 6.1: In 3D space, general rotations depend on three parameters, but a vector undergoing such rotation is restricted to a two dimensional surface.

The $\mathfrak{su}(3)$ algebra is also equipped with a cubic Casimir invariant

$$C_3 = \sum_{i,j,k} d_{abc}\lambda_a\lambda_b\lambda_c, \tag{6.20}$$

corresponding to a trilinear invariant form

$$T(X,Y,Z) = \sum_{a,b,c=1}^{8} d_{abc}x_a y_b z_c = \vec{x}\cdot(\vec{y}\star\vec{z}). \tag{6.21}$$

In particular, the "cubic norm" $\vec{h}\cdot\vec{h}\star\vec{h}$ of any Hamiltonian stays invariant under any unitary transformation.

Those two restrictions point to the fact that a Hamiltonian undergoing a unitary transformation cannot span the full eight-dimensional space. Instead, it stays on a surface, called *orbit*, which is at most six dimensional.

6.1.1 Orbits

The $SU(3)$ group is 8-dimensional. However, the Hamiltonian under arbitrary SU(3) transformations does not explore the full 8D space. Instead, it stays within a lower-dimensional subspace called **orbit**. [13] This is similar to the fact that, by rotating a particular 3D vector, it can only orbit 2D space, as illustrated in Fig. 6.1.

The orbit of a Hamiltonian in vector form (as an 8-dimensional vector $\vec{h}$) is defined as the set

$$\{\vec{h}'|\vec{h}'\cdot\vec{\lambda} = U^\dagger\vec{h}\cdot\vec{\lambda}U, U\in SU(3)\} \tag{6.22}$$

of the Hamiltonians acquired after transforming $\vec{h}\cdot\vec{\lambda}$ with any possible $SU(3)$ transformation U. Although U in general is eight dimensional, the orbits are a subspace of the

$\mathfrak{su}(3)$ algebra, which can be either six-dimensional or four-dimensional, as we will see later.

The concept of orbits is useful as it can simplify the computational analysis. Consider a Hamiltonian with time-independent eigenenergies. For example, this is the case for a Floquet Hamiltonian, whose quasienergies do not depend on time. Suppose the Floquet Hamiltonian always lies in a six-dimensional space. To transform it to a time-independent matrix, we need a transformation depending on only six parameters. The AGP corresponding to such transformation depends on only six parameters as well. Therefore, when looking for an AGP associated with our Hamiltonian, we can restrict our search to a subspace of all possible gauge potentials requiring fewer than eight parameters. Such parametrization is found in Sec. 6.3.

To find the structure of the orbits more precisely, we can represent each orbit with its diagonal element. Indeed, for each Hamiltonian, there exists a matrix U that diagonalizes it. Therefore, there is a diagonal Hamiltonian in each orbit. Let it be $\vec{h} = h\vec{n}$, where $|\vec{n}| = 1$. The diagonal matrix $\vec{n}\cdot\vec{\lambda}$ has only λ_3 and λ_8 components, so we can write $\vec{n}\cdot\vec{\lambda}$ as [13]

$$\begin{aligned}\vec{n}\cdot\vec{\lambda} &= \cos\theta\lambda_3 + \sin\theta\lambda_8 \\ &= \operatorname{diag}\left(\cos\theta + \frac{\sin\theta}{\sqrt{3}}, -\cos\theta + \frac{\sin\theta}{\sqrt{3}}, -\frac{2}{\sqrt{3}}\sin\theta\right)\end{aligned} \tag{6.23}$$

The special cases $\theta = \pi/2$ and $\theta = \pi/6$ respectively correspond to orbits of degenerate Hamiltonians

$$\vec{n}\cdot\vec{\lambda} = \operatorname{diag}\left(\frac{1}{\sqrt{3}}, \frac{1}{\sqrt{3}}, -\frac{2}{\sqrt{3}}\right) \quad \text{and} \quad \vec{n}\cdot\vec{\lambda} = \operatorname{diag}\left(\frac{2}{\sqrt{3}}, -\frac{1}{\sqrt{3}}, -\frac{1}{\sqrt{3}}\right). \tag{6.24}$$

Let us first look at the generic case $\theta \in (\pi/6, \pi/2)$. We start by parametrizing $U^\dagger \in SU(3)$ with the Cartan decomposition (6.11). The subgroup $U(1)\times U(1) = \{e^{i\lambda_3 c}e^{i\lambda_8\phi}\}$ is the centralizer of the diagonal Hamiltonian, because it commutes with λ_3 and λ_8:

$$e^{i\lambda_3 c}e^{i\lambda_8\phi}He^{-i\lambda_8\phi}e^{-i\lambda_3 c} = H. \tag{6.25}$$

After removing these rotations as redundant, we are left with exactly (6.12), which stays inside the six dimensional coset space $\mathscr{S} = SU(3)/U(1)\times U(1)$. Finally, the orbit of H is isomorphic to $U \in SU(3)/U(1)\times U(1)$ (each element of the orbit corresponds to a matrix in the form (6.12)).

We now turn our attention to the degenerate orbits. If $\theta = \pi/2$, $\vec{n}\cdot\vec{\lambda} = \lambda_8$, which commutes with the whole $U(2)$ group generated by λ_1, λ_2, λ_3, λ_8. If we parametrize U in the same way as before, we can remove the whole rotation

$$e^{i\lambda_3 a}e^{i\lambda_2 b}e^{i\lambda_3 c}e^{i\lambda_8\phi}He^{-i\lambda_2 b}e^{-i\lambda_3 a}e^{-i\lambda_8\phi}e^{-i\lambda_3 c} = H, \tag{6.26}$$

leaving us with exactly (6.13), which are the elements of the four dimensional coset space $\mathscr{R} = SU(3)/U(2)$.

The other degenerate orbit $\theta = \pi/6$ has the same algebraic structure as $\theta = \pi/2$ – the orbit is isomorphic to $SU(3)/U(2)$. To get a parametrization of U without any redundancies, we will change our initial parametrization with

$$U = e^{iH_2\alpha}e^{i\lambda_7\beta}e^{iH_2\gamma}e^{-i\lambda_2\theta}e^{iH_2 a}e^{i\lambda_7 b}e^{iH_2 c}e^{i(-\lambda_8/2-\lambda_3\sqrt{3}/2)\phi}, \tag{6.27}$$

where we have made permutations $(1,2,3) \to (3,1,2)$ to the rows and columns of all matrices in (6.11).

In this decomposition, λ_7, H_2 and $\lambda_8/2 + \lambda_3\sqrt{3}/2$ commute with $\vec{n}\cdot\vec{\lambda}$, and dropping the corresponding exponentials gives us the four-parameter rotation

$$U_{\mathscr{R}} = e^{iH_2\alpha}e^{i\lambda_7\beta}e^{iH_2\gamma}e^{-i\lambda_2\theta}. \tag{6.28}$$

6.2 Adiabatic Gauge Potential Parametrization

In the quest of finding gauge potentials for particular systems, it is useful to know the most general form such gauge potential can take. For example, if we try to find the gauge potential variationally, we can restrict our ansatz only to the set of theoretically possible gauge potentials. When seeking such variational AGP, we need it to be parametrized correctly, so that we can variationally search for the values of the paraemters.

To get a parametrization of the gauge potential, we take advantage of the Cartan decomposition from Eq. (6.11). Its corresponding AGP is

$$\mathcal{A} = i\dot{U}U^\dagger = \dot{\alpha}\mathcal{A}_\alpha + \dot{\beta}\mathcal{A}_\beta + \dot{\gamma}\mathcal{A}_\gamma + \dot{\theta}\mathcal{A}_\theta + \dot{a}\mathcal{A}_a + \dot{b}\mathcal{A}_b + \dot{c}\mathcal{A}_c + \dot{\phi}\mathcal{A}_\phi. \tag{6.29}$$

We list the expressions for each component of the gauge potential. To make the expressions more compact, we define a function

$$\rho_{ij}(x) = \cos x\lambda_i + \sin x\lambda_j, \tag{6.30}$$

$$\mathcal{A}_\alpha = -\lambda_3, \tag{6.31}$$

$$\mathcal{A}_\beta = -\rho_{21}(2\alpha), \tag{6.32}$$

$$\mathcal{A}_\gamma = \sin 2\beta\rho_{12}(-2\alpha) - \cos 2\beta\lambda_3, \tag{6.33}$$

$$\mathcal{A}_\theta = -\cos\beta\rho_{54}(\alpha+\gamma) + \sin\beta\rho_{76}(-\alpha+\gamma), \tag{6.34}$$

$$\begin{aligned}\mathcal{A}_a =& \frac{1}{2}((1+\cos^2\theta)\mathcal{A}_\gamma \\ &+ \sin 2\theta\cos\beta\rho_{45}(-\alpha-\gamma) \\ &- \sin 2\theta\sin\beta\rho_{67}(\alpha-\gamma) \\ &+ \sqrt{3}\sin^2\theta\lambda_8),\end{aligned}$$

$$\begin{aligned}\mathcal{A}_b =& -\cos\theta\sin(2(a+\gamma))(\cos 2\beta\rho_{12}(-2\alpha) + \sin 2\beta\lambda_3) \\ &- \cos\theta\cos(2(a+\gamma))\rho_{21}(2\alpha) \\ &- \sin\theta\sin\beta\rho_{54}(-2a+\alpha-\gamma) \\ &- \sin\theta\cos\beta\rho_{76}(-2a-\alpha-\gamma),\end{aligned} \tag{6.35}$$

$$\mathcal{A}_c = \cos 2b\mathcal{A}_a + \sin 2b\mathcal{A}_b \left(a \leftarrow a - \frac{\pi}{4}\right) \tag{6.36}$$

$$\mathcal{A}_\phi = \sqrt{3}\mathcal{A}_a - \sqrt{3}A_\gamma - \lambda_8. \tag{6.37}$$

We also provide the full matrix form of the gauge potential components in App. B.

The expression we obtained also represents the most general form of a pure micromotion drive. This is a class of drives in Floquet theory discussed in Sec. 3.2.1. A Floquet system driven only by the gauge potential $\mathcal{A}$ has Floquet Hamiltonian $H_F = 0$. Such systems do not absorb energy from the drive, preventing heating and maintaining minimal nonequilibrium properties [6].

6.3 Adiabatic Gauge Parametrization along Orbits

We can take advantage of the orbits discussed in Sec. 6.1.1 to simplify our AGP parametrization. If a Hamiltonian has constant eigenenergies (e.g., the Floquet Hamiltonian), it lives in a four or six dimensional subspace of the 8-dimensional $\mathfrak{su}(3)$. To find the appropriate couterdiabatic drive, we can restrict our search to a subspace of all possible gauge potentials as well.

First, consider the case where the Hamiltonian is non-degenerate. It lives in the $\mathscr{I} = SU(3)/U(1) \times U(1)$ orbit. This means, as discussed in Sec. 6.1.1, it can be diagonalized by the six-parameter rotation matrix

$$U_{\mathscr{I}} = e^{i\lambda_3\alpha}e^{i\lambda_2\beta}e^{i\lambda_3\gamma}e^{i\lambda_5\theta}e^{i\lambda_3 a}e^{i\lambda_2 b}. \tag{6.38}$$

Its corresponding AGP lacks the complicated $\mathcal{A}_c$ and $\mathcal{A}_\phi$ components of the general case AGP from Eq. (6.29), taking the form

$$\mathcal{A}_{\mathscr{I}} = i\dot{U}U^\dagger = \dot{\alpha}\mathcal{A}_\alpha + \dot{\beta}\mathcal{A}_\beta + \dot{\gamma}\mathcal{A}_\gamma + \dot{\theta}\mathcal{A}_\theta + \dot{a}\mathcal{A}_a + \dot{b}\mathcal{A}_b, \tag{6.39}$$

where each component satisfies Eq. (6.31) – (6.35).

Now let us consider a Hamiltonian in the degenerate orbit $\mathscr{R} = SU(3)/U(2)$. In the case $\theta = \pi/2$ from Sec. 6.1.1, the rotation matrix reduces to

$$U_{\mathscr{R}} = e^{i\lambda_3\alpha}e^{i\lambda_2\beta}e^{i\lambda_3\gamma}e^{i\lambda_5\theta}, \tag{6.40}$$

meaning that the AGP simplifies to

$$\mathcal{A}_{\mathscr{R}} = i\dot{U}U^\dagger = \dot{\alpha}\mathcal{A}_\alpha + \dot{\beta}\mathcal{A}_\beta + \dot{\gamma}\mathcal{A}_\gamma + \dot{\theta}\mathcal{A}_\theta. \tag{6.41}$$

Again $\mathcal{A}_\alpha$, $\mathcal{A}_\beta$, $\mathcal{A}_\gamma$, $\mathcal{A}_\theta$ are the same potentials as (6.31) – (6.34). As we see, we now need only four parameters to parametrize the AGP.

For the other degenerate orbit $\theta = \pi/6$, everything is analogous up to a permutation of rows and columns of all the matrices:

$$U_{\mathscr{R}} = e^{iH_2\alpha}e^{i\lambda_7\beta}e^{iH_2\gamma}e^{-i\lambda_2\theta}, \tag{6.42}$$

leading to

$$\mathcal{A}_{\mathscr{R}} = i\dot{U}U^\dagger = \dot{\alpha}\mathcal{A}_{\alpha\mathscr{R}2} + \dot{\beta}\mathcal{A}_{\beta\mathscr{R}2} + \dot{\gamma}\mathcal{A}_{\gamma\mathscr{R}2} + \dot{\theta}\mathcal{A}_{\theta\mathscr{R}2}, \tag{6.43}$$

where (6.31) – (6.34) undergo permutations of their rows and columns, leading to

$$\mathcal{A}_\alpha = -H_2, \tag{6.44}$$
$$\mathcal{A}_\beta = -\rho_{76}(2\alpha), \tag{6.45}$$
$$\mathcal{A}_\gamma = \sin 2\beta\rho_{67}(-2\alpha) - \cos 2\beta H_2, \tag{6.46}$$
$$\mathcal{A}_\theta = \cos\beta\rho_{21}(-\alpha-\gamma) - \sin\beta\rho_{54}(\alpha-\gamma). \tag{6.47}$$

6.4 Kato Gauge Potential

In this section, we use the vector notation from Sec. 4.1 to find a direct expression for the Kato gauge potential.

The formula we obtain can be useful even if we want to obtain an arbitrary AGP, as it is a completely different type of expression from the parametrization in Sec. 6.2. An arbitrary gauge AGP can be obtained by adding an operator that commutates with the Hamiltonian.

However, the Kato potential itself is important, as it offers geometric driving. It generates Berry phases, and in the case of degenerate system – holonomies, which are present in the adiabatic evolution.

We assume a three-level system with traceless Hamiltonian. For the formula to work, we need to know the eigenvalues (energies) of the Hamiltonian $E_{1,2,3}$ in advance.

Our formula relies on the projector-based definition of the Kato AGP (2.37), so we start by turning the projectors to a vector form. The projectors can be expressed [8] as

$$\Pi_\alpha = \frac{1}{3E_\alpha^2 - \frac{C_2}{2}} \left(\left(E_\alpha^2 - \frac{C_2}{2} \right) \mathbf{1}_3 + E_\alpha H + H^2 \right), \tag{6.48}$$

where

$$C_n \equiv \mathrm{Tr}(H^n) = \sum_{\alpha=1}^{N} E_\alpha^n \tag{6.49}$$

is the n-th Casimir invariant.

Next, we turn $H = \vec{h} \cdot \vec{\lambda}$, and express H^2 as a star product:

$$H^2 = \frac{1}{2}\{H, H\} = \frac{2}{3}\vec{h} \cdot \vec{h} + (\vec{h} \star \vec{h}) \cdot \vec{\lambda} = \frac{2}{3}C_2 + (\vec{h} \star \vec{h}) \cdot \vec{\lambda}. \tag{6.50}$$

The projector now takes the form [8]

$$\Pi_\alpha = \frac{1}{3}\mathbf{1}_3 + \frac{1}{2}\vec{b}_\alpha \cdot \vec{\lambda}, \tag{6.51}$$

where

$$\vec{b}_\alpha = \frac{2}{3E_\alpha^2 - \frac{C_2}{2}}(E_\alpha \vec{h} + \vec{h} \star \vec{h}). \tag{6.52}$$

In vector notation, $C_2 = 2\vec{h} \cdot \vec{h}$.

We can first express $\mathcal{A}^K$ in terms of $\vec{b}$ and $\dot{\vec{b}}$:

$$\begin{aligned} \mathcal{A}^K &= \frac{1}{2}\sum_\alpha [i\dot{\Pi}_\alpha, \Pi_\alpha] \\ &= \frac{i}{2}\sum_\alpha \left[\frac{1}{2}\dot{\vec{b}}_\alpha \cdot \vec{\lambda}, \frac{1}{3}\mathbf{1}_3 + \frac{1}{2}\vec{b}_\alpha \cdot \vec{\lambda} \right] \\ &= -\sum_\alpha \frac{\dot{\vec{b}}_\alpha}{2} \times \frac{\vec{b}_\alpha}{2}. \end{aligned} \tag{6.53}$$

Next, we compute $\dot{\vec{b}}$:

$$\dot{\vec{b}}_\alpha = \frac{2}{\left(3E_\alpha^2 - \frac{C_2}{2}\right)^2}\left(\left(6E_\alpha\dot{E}_\alpha - \frac{\dot{C}_2}{2}\right)\left(E_\alpha\vec{h} + \vec{h}_\star\right) + \left(3E_\alpha^2 - \frac{C_2}{2}\right)\left(\dot{E}_\alpha\vec{h} + E_\alpha\dot{\vec{h}} + \dot{\vec{h}}_\star\right)\right), \tag{6.54}$$

where $\vec{h} \star \vec{h}$ is denoted $\vec{h}_\star$ to get more compact expressions.

When multiplying $\dot{\vec{b}}_\alpha \times \vec{b}_\alpha$, note that

$$(E_\alpha\vec{h} + \vec{h}_\star) \times (E_\alpha\vec{h} + \vec{h}_\star) = 0, \tag{6.55}$$

which finally gives

$$\mathcal{A}_\lambda^K = -\sum_\alpha \frac{(E_\alpha\dot{\vec{h}} + \dot{\vec{h}}_\star) \times (E_\alpha\vec{h} + \vec{h}_\star) + \dot{E}_\alpha\vec{h} \times \vec{h}_\star}{(3E_\alpha^2 - \frac{C_2}{2})^2} \cdot \vec{\lambda}. \tag{6.56}$$

If the eigenenergies of the system are constant, (6.56) simplifies to

$$\mathcal{A}_\lambda^K = -\sum_\alpha \frac{(E_\alpha\dot{\vec{h}} + \dot{\vec{h}}_\star) \times (E_\alpha\vec{h} + \vec{h}_\star)}{(3E_\alpha^2 - \frac{C_2}{2})^2} \cdot \vec{\lambda}. \tag{6.57}$$

6.5 Kato Gauge Potential with Degeneracy

In degenerate three-level systems, Eq. (6.56) diverges and no longer produces a valid Kato AGP.

Let E_1 and E_2 be the degenerate energy levels, so that $E_1 = E_2 = E$, $E_3 = -2E$, $C_2 = 6E^2$. The denominator at $\alpha = 1$ is now

$$\left(3E_1^2 - \frac{C_2}{2}\right)^2 = 0. \tag{6.58}$$

The problem arises from the fact that we derive the Kato AGP from the projectors, but in the case of a degeneracy, the projectors are not defined for individual states. Instead, the projector on the degenerate eigenspace is

$$\Pi_{12} = |\psi_1\rangle\langle\psi_1| + |\psi_2\rangle\langle\psi_2|. \tag{6.59}$$

The projectors can be expressed by the Hamiltonian as

$$\Pi_{12} = \frac{2E + H}{3E} \tag{6.60}$$

and

$$\Pi_3 = \frac{E - H}{3E}. \tag{6.61}$$

Eq. (6.51) still holds for Π_3. Our new equation looks simpler – it is linear in H. In fact, it is the same projector as (6.51). If we use $\Pi_3^2 = \Pi_3$ and square the new expression, we would get exactly(6.51). Again, we write the projectors in vector notation:

$$\Pi_{12} = \frac{2}{3} + \frac{\vec{h} \cdot \vec{\lambda}}{3E} \tag{6.62}$$

$$\Pi_3 = \frac{1}{3} - \frac{\vec{h}\cdot\vec{\lambda}}{3E} \tag{6.63}$$

Now, we assume that our system remains degenerate along the drive trajectory in parameter space. This will be true for Floquet systems, whose quasienergies do not change. However, our assumption is weaker in the sense that it allows changes of the energy E. We calculate the derivatives of the projectors:

$$\dot{\Pi}_{12} = \frac{1}{3E}\dot{\vec{h}}\cdot\vec{\lambda} - \frac{\dot{E}}{3E^2}\vec{h}\cdot\vec{\lambda}, \tag{6.64}$$

$$\dot{\Pi}_3 = -\frac{1}{3E}\dot{\vec{h}}\cdot\vec{\lambda} + \frac{\dot{E}}{3E^2}\vec{h}\cdot\vec{\lambda} \tag{6.65}$$

and plug them in the expression of the Kato AGP:

$$\begin{aligned}
\mathcal{A}^K &= \frac{1}{2}\sum_\alpha [i\dot{\Pi}_\alpha, \Pi_\alpha] \\
&= -\left(\left(\frac{1}{3E}\dot{\vec{h}} - \frac{\dot{E}}{3E^2}\vec{h}\right)\times\frac{\vec{h}}{3E} + \left(-\frac{1}{3E}\dot{\vec{h}}\cdot\vec{\lambda} + \frac{\dot{E}}{3E^2}\vec{h}\right)\times\left(-\frac{\vec{h}}{3E}\right)\right)\cdot\vec{\lambda} \\
&= -\left(\left(\frac{1}{3E}\dot{\vec{h}}\right)\times\frac{\vec{h}}{3E} + \left(-\frac{1}{3E}\dot{\vec{h}}\right)\times\left(-\frac{\vec{h}}{3E}\right)\right)\cdot\vec{\lambda} \\
&= -\frac{2\dot{\vec{h}}\times\vec{h}}{9E^2}\cdot\vec{\lambda}
\end{aligned} \tag{6.66}$$

Why are the degenerate gauge potentials different?

By definition, gauge potentials do not know about the energy of the system – they are only based on the eigenstates. If, however, two of the energy levels overlap, the eigenstates of the degenerate energy level are not uniquely defined. A general (not necessarily Kato) AGP can be obtained via multiple possible unitary transformations. In other words, the degenerate energy level gives us an additional gauge freedom for constructing gauge potentials.

Specifically, the Kato AGP fixes all the gauge freedoms. In the non-degenerate case, its diagonal elements in the Hamiltonian's eigenbasis are set to zero. In the degenerate case, however, all of its elements in the degenerate subspace are set to zero. Evolution with the Kato AGP now includes holonomic transitions between the degenerate eigenstates. In contrast, evolution with a Kato AGP obtained from a non-degenerate Hamiltonian will not allow such transitions.

Chapter 7

Counter-Diabatic Driving for Periodically Driven Three Level Systems

This chapter brings together the theoretical concepts in numerical simulations to address our central goal: designing counter-diabatic drives for periodically driven three-level systems. First, we find the counter-diabatic drive of a Λ-type system driven by an oscillatory periodic field. We show that the variational method from Chapter 4.2.3 produces a high-fidelity counter-diabatic drive at various frequencies. Next, we tackle the scenario of a system with degenerate states, deriving the Kato gauge potential with our compact formula from Sec. (6.5). We compare the evolution of the degenerate system, showing that the evolution with the Kato AGP produces holonomic transition, and the adiabatic evolution adds dynamical phases to the evolution. Finally, we outline how to construct geometric gates, e.g. controlled-Z gate (a two-qubit entangling gate) using a three-level system as an intermediary.

7.1 Example: Lambda System

In this section, we use the variational method to find the Floquet Hamiltonian of a periodically driven Λ- system.

A Λ three-level configuration contains two low-energy states $|0\rangle, |1\rangle$ and one excited state $|e\rangle$. This is one of the most common configurations in atomic physics and quantum optics. It has also been used in quantum control experiments [14]. In our analysis, we add an interaction term (coupling) to split the degeneracy between $|0\rangle$ and $|1\rangle$, as shown in Fig. 7.1. This is also common in experiments [15]. For a general multi-level atom or molecule, interacting with an electromagnetic field, such splitting is known as AC Stark effect. The effective eigenstates of such photon-atom system are known as "dressed states" [16]. The full understanding of dressed states requires viewing the electromagnetic field as a quantum field, which is beyond the scope of this thesis.

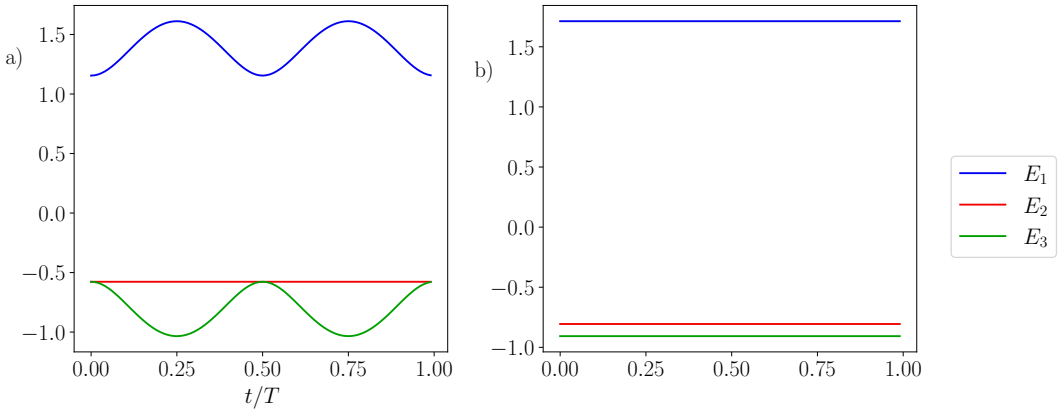

Figure 7.1: Eigenenergies of a) the Hamiltonian; b) the Floquet Hamiltonian of the lambda system at $\omega/\Delta = 4$, $g/\Delta = 1$. When the driving term is zero, the Hamiltonian has a degeneracy; the Floquet Hamiltonian has constant energies and is not degenerate.

Problem Setup

Our quantum system has ground states $|0\rangle$, $|1\rangle$ and an excited state $|e\rangle$ with energy gap Δ interacting with a periodic field (e.g. laser field) of strength g with frequency ω. The Hamiltonian of the system reads

$$H(t) = -\Delta\lambda_8 + g\sin\omega t\,(\lambda_4 + \lambda_6)\,, \tag{7.1}$$

where λ_8 discriminates the ground states from the excited state, λ_4 couples $|0\rangle$ to $|e\rangle$ and λ_6 couples $|1\rangle$ to $|e\rangle$.

Without the interaction term, the ground states have identical energy. However, by adding the interaction, all three eigenstates have distinct energies, cf. Fig. 7.1.

Variational Method

Similar to Sec. 5.4, we can't give an analytical solution for the evolution of the system. Therefore, as a baseline for evaluating the variational AGP, we first solve Schrodinger's equation numerically over one period to construct the Floquet unitary U_F. Then, we take matrix log to find the Floquet Hamiltonian H_F inside the Floquet zone.

On the other hand, we search for a gauge potential variationally, as in Sec. 4.2.2. We start with an ansatz for the kick operator K and minimize the action $S = \mathrm{Tr}(G^2)$ using the modified gradient descent from Sec. 4.2.3. Then, to compare the results with the numerical integration, we calculate the Floquet Hamiltonian

$$H_F = H - \mathcal{A}_F. \tag{7.2}$$

We do this for different driving frequencies, showing the robustness of the variational method to work properly in both low- and high-frequency settings.

At different frequencies, the Floquet Hamiltonian obtained lies in different Floquet zones. To make the comparison between the numerical integration and the variationally obtained gauge, we plotted the numerical Floquet Hamiltonian in Fig. 7.2 corresponding to the same Floquet zone as the variationally obtained.

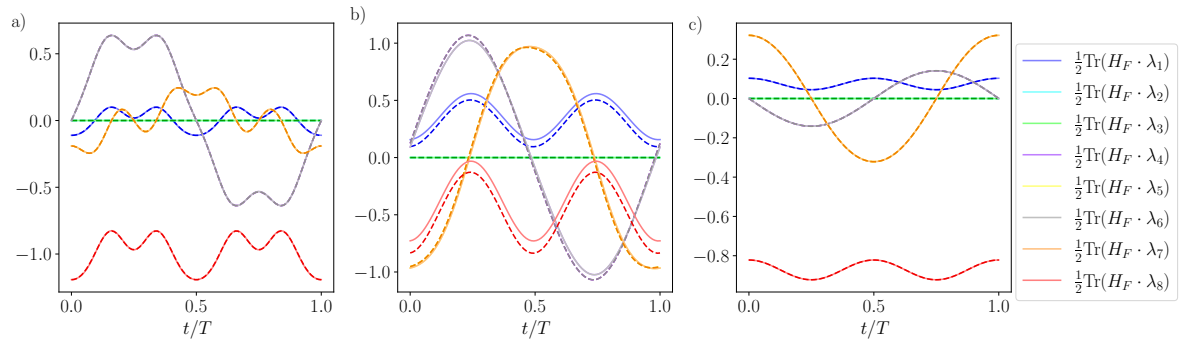

Figure 7.2: Floquet Hamiltonian components in the Gell-Mann basis vs initial time. Found using the variational method (solid line) vs numerical integration and matrix log (dashed line) for a) $\omega/\Delta = 0.5$, b) $\omega/\Delta = 2$, c) $\omega/\Delta = 4$. The variational algorithm in b) has not yet converged. The Floquet Hamiltonian in c) is the principal log of the Floquet unitary, while a) and b) converged to a higher "Floquet zone". Some components are equivalent (see text). For all simulations, $g/\Delta = 1$. Number of harmonic used: a) 6; b) 3; c) 3. The variational algorithm, when fully converged, provides a high-fidelity AGP.

In general, the variational method converges nearly perfectly, so the difference between the Floquet Hamiltonians cannot be noticed in the figure. We have left one of the experiments (at frequency $\omega/\Delta = 2$) in a state before the full convergence of the algorithm, showing differences with the "theory".

Another feature of Fig. 7.2 is that due to the symmetry of the problem, some components of the Floquet Hamiltonian coincide. Although all of the components

$$h_i = \frac{1}{2}\mathrm{Tr}(H \cdot \lambda_i) \iff H = \sum_i h_i \lambda_i \tag{7.3}$$

are plotted, we cannot see all components on the plot, because $h_2 = h_1$, $h_4 = h_6$ and $h_5 = h_7$.

7.2 Example: Holonomy

In this section, we explore the adiabatic evolution of a degenerate three-level system. We show that it leads to a non-Abelian holonomy instead of simple Berry phases. We test our formula for the degenerate Kato gauge potential (6.66) and show that driving with the Kato AGP only generates the holonomy matrix.

To manufacture a three-level-system Hamiltonian with degenerate energy levels, we start with

$$\lambda_8 = \frac{1}{\sqrt{3}}\mathrm{diag}(1, 1, -2) \tag{7.4}$$

and rotate it with a unitary matrix P to get

$$H = P\lambda_8 P^\dagger. \tag{7.5}$$

We make an almost arbitrary choice

$$P(t) = e^{-i\frac{\pi}{6}(\lambda_4 \sin\omega t + \lambda_7 \cos\omega t)}, \tag{7.6}$$

where the "direction of rotation" $\lambda_4 \sin\omega t + \lambda_7 \cos\omega t$ is changing periodically and λ_4, λ_7 and λ_8 do not create a distinct subalgebra of $SU(3)$, so the Hamiltonian is tracing a generic path in $SU(3)$.

This system is simple enough to calculate a lot of its characteristics analytically.

Since we already know the transformation P that diagonalizes the Hamiltonian, the AGP of the system is

$$\mathcal{A}^U = i\dot{P}P^\dagger = \omega\left(\frac{\sqrt{3}}{2} - 1\right)\lambda_1 + \omega\frac{\cos(\omega t)}{2}\lambda_4 - \omega\frac{\sin(\omega t)}{2}\lambda_7. \tag{7.7}$$

In addition, we can calculate the Kato AGP using the vector formula

$$\frac{1}{2}\mathrm{Tr}(\mathcal{A}^K \cdot \vec{\lambda}) = -2\frac{\dot{\vec{h}} \times \vec{h}}{9E^2}, \tag{7.8}$$

where

$$\vec{h} = \frac{1}{2}\mathrm{Tr}(H \cdot \vec{\lambda}) = \left(0, \frac{\sqrt{3}}{8}\sin(2\omega t), \frac{\sqrt{3}}{8}\cos(2\omega t), 0, -\frac{3}{4}\sin(\omega t), \frac{3}{4}(\omega t), 0, \frac{5}{8}\right). \tag{7.9}$$

Applying the vector formula, we get the Kato AGP

$$\begin{aligned} \vec{a}_K &= \left(-\frac{\omega}{4}, 0, \frac{\sqrt{3}}{4}\omega\cos(\omega t), 0, 0, -\frac{\sqrt{3}}{4}\omega\sin(\omega t), 0\right) \\ \Rightarrow \mathcal{A}^K &= -\frac{\omega}{4}\lambda_1 + \frac{\sqrt{3}}{4}\omega\cos(\omega t)\lambda_4 - \frac{\sqrt{3}}{4}\omega\sin(\omega t)\lambda_7 \end{aligned} \tag{7.10}$$

In the rotating reference frame,

$$\begin{aligned} \tilde{\mathcal{A}}^U &= \omega\left(1 - \frac{\sqrt{3}}{2}\right)\lambda_1 + \frac{\omega}{2}\left(\cos(\omega t)\lambda_4 - \sin(\omega t)\lambda_7\right) \\ \tilde{\mathcal{A}}^K &= \frac{\omega}{2}\left(\cos(\omega t)\lambda_4 - \sin(\omega t)\lambda_7\right). \end{aligned} \tag{7.11}$$

For a non-degenerate Hamiltonian, the Kato AGP has no diagonal elements. For a degenerate Hamiltonian, in addition, there should be no elements in the whole 2×2 block of the degenerate energy levels. In this example,

$$\begin{aligned} \tilde{\mathcal{A}}^U &= \frac{\omega}{2}\begin{pmatrix} 0 & 2-\sqrt{3} & \cos(\omega t) \\ 2-\sqrt{3} & 0 & -i\sin(\omega t) \\ \cos(\omega t) & i\sin(\omega t) & 0 \end{pmatrix}, \\ \tilde{\mathcal{A}}^K &= \frac{\omega}{2}\begin{pmatrix} 0 & 0 & \cos(\omega t) \\ 0 & 0 & -i\sin(\omega t) \\ \cos(\omega t) & i\sin(\omega t) & 0 \end{pmatrix}, \end{aligned} \tag{7.12}$$

confirming that $\tilde{\mathcal{A}}^K$ has no elements in the 2×2 block and on the main diagonals, while all other elements are the same as in $\tilde{\mathcal{A}}^U$. The difference between $\tilde{\mathcal{A}}^K$ and $\tilde{\mathcal{A}}^U$ is

$$\tilde{\mathcal{A}}^U - \tilde{\mathcal{A}}^K = \omega\left(1 - \frac{\sqrt{3}}{2}\right)\lambda_1 = \frac{\omega}{2}\begin{pmatrix} 0 & 2-\sqrt{3} & 0 \\ 2-\sqrt{3} & 0 & 0 \\ 0 & 0 & 0 \end{pmatrix}. \tag{7.13}$$

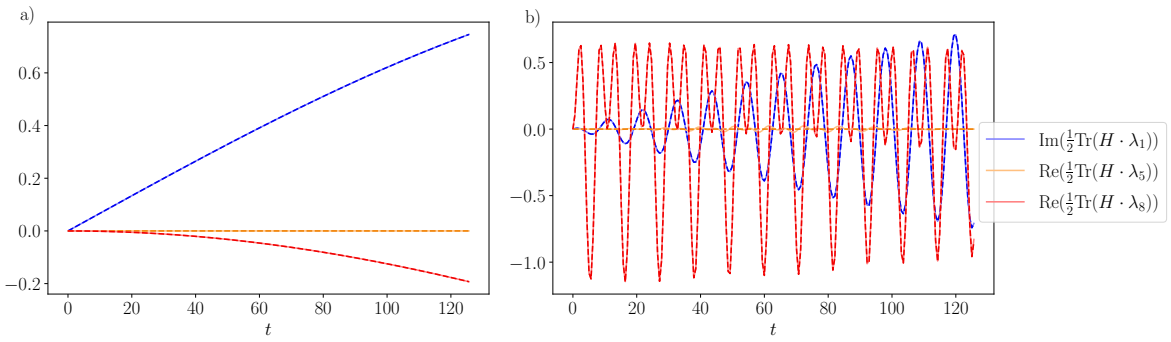

Figure 7.3: Comparison between a) the evolution obtained by integrating the Kato AGP (solid line) vs the holonomy matrix (dashed line); b) the adiabatic evolution (solid line) vs the dynamic phases + holonomy (dashed line). Parameters in the simulation: $\omega = 0.05$. The Berry connections generate the correct adiabatic evolution. Imperfect adiabaticity leads to small deviations from the holonomic evolution.

Because of the degeneracy, instead of Berry phases, we have a matrix of Berry connections – the 2×2 block of $\tilde{\mathcal{A}}^U - \tilde{\mathcal{A}}^K$, corresponding to the degenerate level:

$$A = \frac{\omega}{2} \begin{pmatrix} 0 & 2-\sqrt{3} \\ 2-\sqrt{3} & 0 \end{pmatrix} = \left(1 - \frac{\sqrt{3}}{2}\right) \sigma_1. \tag{7.14}$$

It generates a 2×2 holonomy matrix

$$W = e^{iAt}. \tag{7.15}$$

In the general case, the third energy level could also accumulate a Berry phase.

We perform two numerical simulations showing the impact of holonomy on the evolution of the system. First, we compute the pure geometric evolution as a time-ordered exponent of the Kato Hamiltonian:

$$U^K = P^\dagger(t)\, \mathcal{T} \exp\left(-i \int_0^t \mathcal{A}^K dt\right) P(0), \tag{7.16}$$

and compare it with the holonomy matrix. The results are shown in Fig. 7.3 a.

Then, we evolve the system adiabatically:

$$U = \exp\left(-i \int_0^t H(t')dt'\right). \tag{7.17}$$

In the rotating reference frame, the evolution takes the form

$$U_{\text{rot}} = P^\dagger(t) U(t,0) P(0). \tag{7.18}$$

In the adiabatic limit, the evolution must match the accumulation of dynamic phases and a holonomy

$$U_{\text{rot}} \approx \begin{pmatrix} W & & 0 \\ & & 0 \\ 0 & 0 & 1 \end{pmatrix} \begin{pmatrix} e^{-iE_1 t} & 0 & 0 \\ 0 & e^{-iE_2 t} & 0 \\ 0 & 0 & e^{-iE_3 t} \end{pmatrix}, \tag{7.19}$$

where E_1, E_2, E_3 in our system are the diagonal elements of λ_8. Fig. 7.3 b compares both approaches to compute the evolution. Since the system is evolving slowly, but

is not exactly in the adiabatic limit, we can notice small deviations from the theoretical evolution. To make the figures clearer, we have omitted most components of the evolution matrices. The missing components have analogous behavior.

7.3 Example: Geometric Quantum Logic Gate

One of the important aspects in the development of quantum computers is the construction of high-fidelity gates. In particular, two qubit gates typically have lower fidelity, while they are critical for the performance of all quantum algorithms. For example, the CZ gates must meet the fault-tolerance threshold for quantum error correction to be able to work at all – otherwise it would produce more errors than it tries to correct.

We suggest a scheme for executing a pure geometric CZ quantum gate within the framework of 3LS.

The CZ gate has the form

$$CZ = \begin{pmatrix} 1 & 0 & 0 & 0 \\ 0 & 1 & 0 & 0 \\ 0 & 0 & 1 & 0 \\ 0 & 0 & 0 & -1 \end{pmatrix}, \tag{7.20}$$

acting in the computational basis ($|00\rangle$, $|01\rangle$, $|10\rangle$, $|11\rangle$). In a spin qubit quantum computer ($|0\rangle = |\uparrow\rangle$, $|1\rangle = |\downarrow\rangle$), we can directly reduce this gate to a unitary of a 3LS in the subspace here the total spin is $S = 1$.

Let S be the magnitude of the total spin, and m_s – the projection along the magnetic field. The addition of the two spins gives rise to a singlet state

$$|S = 0, m_S = 0\rangle = \frac{1}{\sqrt{2}} \left(|\downarrow\uparrow\rangle - |\uparrow\downarrow\rangle \right), \tag{7.21}$$

which is not affected by the CZ gate, and a triplet state

$$\begin{aligned} |S = 1, m_S = 1\rangle &= |\uparrow\uparrow\rangle \\ |S = 1, m_S = 0\rangle &= \frac{1}{\sqrt{2}} \left(|\downarrow\uparrow\rangle + |\uparrow\downarrow\rangle \right) \\ |S = 1, m_S = -1\rangle &= |\downarrow\downarrow\rangle . \end{aligned} \tag{7.22}$$

In the subspace of the triplet state, the CZ-gate takes the form

$$CZ_{S=1} = \begin{pmatrix} 1 & 0 & 0 \\ 0 & 1 & 0 \\ 0 & 0 & -1 \end{pmatrix}. \tag{7.23}$$

We aim to construct the gate by using a *periodic pure geometric drive*, discussed in Sec. 3.2.1.

We should find the Kato gauge potentials $\mathcal{A}_K$ in the the triplet subspace, such that the pure geometric evolution would produce a CZ gate:

$$CZ_{S=1} = \mathcal{T} \exp\left(-i \int_0^T \mathcal{A}_K(t') dt' \right) = e^{-iH_F T}. \tag{7.24}$$

However, we encounter a problem: the Kato AGP has no diagonal elements in the eigenbasis, therefore is always a traceless operator (it is always in the $\mathfrak{su}(3) \subset \mathfrak{u}(3)$ algebra), and therefore its exponent always has determinant 1 (it is in the $SU(3) \subset U(3)$ group). This means we cannot implement the CZ-gate by purely geometric drive.

One way to fix this problem is instead to make a $-CZ$ gate instead of a CZ gate. In the triplet manifold,

$$-CZ_{S=1} = \begin{pmatrix} -1 & 0 & 0 \\ 0 & -1 & 0 \\ 0 & 0 & 1 \end{pmatrix}. \tag{7.25}$$

Note that in addition to the $-CZ_{S=1}$ gate, which now in theory can be implemented with a pure geometric drive, to implement a full $-CZ$ gate, we have to change the phase of the singlet state as well.

The general Floquet Hamiltonian generating the $-CZ$ gate has the form

$$H_F[0] = \omega \begin{pmatrix} M & & 0 \\ & & 0 \\ 0 & 0 & k \end{pmatrix}, \tag{7.26}$$

where $\omega = 2\pi/T$, $k \in \mathbb{Z}$ and $e^{2\pi i M} = -\mathbf{1} = e^{i\pi}\mathbf{1}$. The latter condition is satisfied by matrices $M = \vec{n} \cdot \vec{\sigma} + l + \frac{1}{2}$, where $|\vec{n}| = n \in \mathbb{Z}$ and $l \in \mathbb{Z}$. The diagonal form of $H_F[t]$ is

$$D = V(t)^\dagger H_F[t] V(t) = \omega \begin{pmatrix} l+n+\frac{1}{2} & 0 & 0 \\ 0 & l-n+\frac{1}{2} & 0 \\ 0 & 0 & k \end{pmatrix}, \tag{7.27}$$

where $V(t)$ can reconstruct the micromotion operator

$$P(t) = V(t)V^\dagger(0) \tag{7.28}$$

and is generated by the Floquet gauge potential as well:

$$\mathcal{A}_F = \dot{P}P^\dagger = \dot{V}V^\dagger. \tag{7.29}$$

To find a pure geometric drive,

$$H = \mathcal{A}_K + 0 = \mathcal{A}_F + H_F[t] = i\dot{V}V^\dagger + VDV^\dagger, \tag{7.30}$$

we can use the fact that the Kato AGP must have zeroes as diagonal elements in the eigenbasis of the Floquet Hamiltonian:

$$(V^\dagger \mathcal{A}_K V)_{mm} = 0 = (iV^\dagger \dot{V})_{mm} + D_{mm}. \tag{7.31}$$

This leaves us with a condition on the diagonal elements of the Floquet AGP:

$$\mathcal{A}_{F\,mm} = -D_{mm}. \tag{7.32}$$

By starting with an ansatz for the "kick operator" as in Eq. (4.24), we can compute $\mathcal{A}_F$ approximately with (4.28). The Floquet AGP in the rotating frame is in fact

$$iP^\dagger \dot{P} = -i\dot{P}^\dagger P = -i\frac{d}{dt} e^{-iK(t)} e^{iK(t)}. \tag{7.33}$$

Comparing it with the gauge potential in the lab frame, we can use the same computation as (4.28), but plugging $-K$ instead of K.

Currently, our variational algorithm gets stuck before finding a solution with a pure geometric driving. This leaves the question of finding a working Kato potential variationally still open for further research.

Chapter 8

Conclusion

We demonstrated how counter-diabatic driving can be systematically extended from two-level to three-level systems. The group properties of $SU(3)$ allowed us to simplify the explicit parametrization of a general micromotion drive. The commutation and anticommutation relations allowed us to derive a vector formula for the Kato gauge potential.

The variational principle allowed us to design high-fidelity gauge potentials which can be used as fast driving protocols, representing a shortcut to adiabaticity. The main significance of such experiments is in quantum computing and quantum simulation, where executing CD protocols allows for both faster gate operation – preventing decoherence, and robustness against leakage.

Recent experimental advancements have demonstrated the feasibility of counter-diabatic (CD) driving beyond theoretical models. Notably, CD driving has been successfully implemented in a 9-site synthetic lattice [17]. Additionally, experimental works have shown how CD driving improves state preparation in spin chains [18] and accelerates adiabatic processes in superconducting circuits [19], paving the way for integration into real-world quantum technologies.

In this thesis, we have used a version of the variational principle [2] tailored for Floquet systems, where the Floquet Hamiltonian is unknown. Starting with a periodic Hamiltonian, we obtained variationally a high-fidelity decomposition to a Floquet Hamiltonian and its AGP.

Our analysis of gauge structures can be extended outside the area of quantum control, to other topics in quantum mechanics, which was the main focus of our thesis. For example, it is interesting to research the topological properties of gauge potentials. This can be applied to topological Euler class insulators [20].

In this thesis, we investigated degeneracy in 3LS. We obtained explicit Floquet and Kato gauge potentials for degenerate systems. We confirmed that the adiabatic evolution of such systems introduces holonomies instead of simple Berry phases. Holonomies have importance in the construction of quantum gates, with Holonomic quantum computation being an active area of research [21]. The degenerate subspace also represents a *decoherence-free subspace* [22], which is useful when trying to protect our quantum gates against decoherence.

Outlook – four-level systems and beyond: The logical next step is to tackle four- and higher-level systems. A lot of the methods we used in the thesis can be carried

over to 4LS. The main challenge will be the increased computational complexity. The $\mathfrak{su}(4)$ algebra contains 15 generators instead of 8, meaning that the evolution operators and gauge potentials should depend on 15 parameters, making them more difficult to derive. Again, the concept of orbits can be used to reduce these parameters. The variational principle can be easily generalized to multi-level systems. However, the gradient descent will be more computationally intensive. Four-level systems will feature more interesting structure, with multiple possible degenerate levels, allowing more complicated non-Abelian holonomies.

We outlined an approach for designing a geometric CZ gate, which is also an area for further research. Research for design of two-qubit gates could stay in the context of 3LS if we consider a submanifold of the two-qubit state space, such as the triplet manifold in spin qubit quantum computers.

Appendix A

Algebra of Pauli Matrices

We define the rotation matrices as

$$\begin{aligned} R_k(\theta) &= \exp\left(-i\frac{\theta}{2}\sigma_k\right) = \sum_{n=0}^{\infty}\frac{(-i)^n\theta^n\sigma_k^n}{2^n n!} = \\ &= \sum_{n=0}^{\infty}\frac{(-1)^n\theta^{2n}\mathbf{1}}{2^{2n}(2n)!} + \sum_{n=0}^{\infty}-i\frac{(-1)^n\theta^{2n+1}\sigma_k}{2^{2n+1}(2n+1)!} = \\ &= \cos\left(\frac{\theta}{2}\right)\mathbf{1} - i\sin\left(\frac{\theta}{2}\right)\sigma_k, \end{aligned} \tag{A.1}$$

$$\partial_\phi R_k = -\frac{1}{2}\sin\left(\frac{\phi}{2}\right) - i\frac{1}{2}\cos\left(\frac{\phi}{2}\right)\sigma_k = -\frac{i}{2}R_k\sigma_k \tag{A.2}$$

$$R_k^\dagger\partial_\phi R_k = -\frac{i}{2}\sigma_k \tag{A.3}$$

We make use of the algebra of the Pauli matrices:

$$\begin{aligned} &\sigma_k\sigma_k = 1, \\ &\sigma_x\sigma_y = i\sigma_z, \\ &\{\sigma_x,\sigma_y\} = 0, \\ &\sigma_x\sigma_y\sigma_x = i\sigma_z\sigma_x = -\sigma_y, \\ &\sigma_x\sigma_z\sigma_x = -i\sigma_y\sigma_x = -\sigma_z. \end{aligned} \tag{A.4}$$

We can then find the action of the rotation matrices on the Pauli matrices

$$\begin{aligned} &R_k^{-1}\mathbf{1}R_k = \mathbf{1}, \\ &R_k^{-1}\sigma_k R_k = \sigma_x, \\ &R_x^{-1}\sigma_y R_x = \cos\theta\sigma_y - \sin\theta\sigma_z, \\ &R_x^{-1}\sigma_z R_x = \sin\theta\sigma_y + \cos\theta\sigma_z. \end{aligned} \tag{A.5}$$

In all above equations we can make the cyclic substitution $x \to y, y \to z, z \to x$.

Appendix B

Explicit Matrix Form of the Parametrized SU(3) Adiabatic Gauge Potential

We list the components of the AGP corresponding to the unitary transformation

$$U(\alpha,\beta,\gamma,\theta,a,b,c,\phi) = e^{i\lambda_3\alpha}e^{i\lambda_2\beta}e^{i\lambda_3\gamma}e^{i\lambda_5\theta}e^{i\lambda_3 a}e^{i\lambda_2 b}e^{i\lambda_3 c}e^{i\lambda_8\phi}, \tag{B.1}$$

discused in Sec. 6.2 as matrices:

$$\begin{aligned}
\mathcal{A}_\alpha &= \begin{pmatrix} -1 & 0 & 0 \\ 0 & 1 & 0 \\ 0 & 0 & 0 \end{pmatrix}, \\
\mathcal{A}_\beta &= \begin{pmatrix} 0 & ie^{i2\alpha} & 0 \\ -ie^{-i2\alpha} & 0 & 0 \\ 0 & 0 & 0 \end{pmatrix}, \\
\mathcal{A}_\gamma &= \begin{pmatrix} -\cos 2\beta & e^{i2\alpha}\sin 2\beta & 0 \\ e^{-i2\alpha}\sin 2\beta & \cos 2\beta & 0 \\ 0 & 0 & 0 \end{pmatrix}, \\
\mathcal{A}_\theta &= \begin{pmatrix} 0 & 0 & ie^{i(\alpha+\gamma)}\cos\beta \\ 0 & 0 & -ie^{-i(\alpha-\gamma)}\sin\beta \\ -ie^{-i(\alpha+\gamma)}\cos\beta & ie^{i(\alpha-\gamma)}\sin\beta & 0 \end{pmatrix}, \\
\mathcal{A}_a &= \begin{pmatrix} 1-\cos^2\beta(1+\cos^2\theta) & e^{i2\alpha}\sin 2\beta\frac{1+\cos^2\theta}{2} & e^{i(\alpha+\gamma)}\cos\beta\frac{\sin 2\theta}{2} \\ e^{-i2\alpha}\sin 2\beta\frac{1+\cos^2\theta}{2} & 1-\sin^2\beta(1+\cos^2\theta) & -e^{-i(\alpha-\gamma)}\sin\beta\frac{\sin 2\theta}{2} \\ e^{-i(\alpha+\gamma)}\cos\beta\frac{\sin 2\theta}{2} & -e^{i(\alpha-\gamma)}\sin\beta\frac{\sin 2\theta}{2} & -\sin^2\theta \end{pmatrix},
\end{aligned} \tag{B.2}$$

$$\begin{aligned}
\mathcal{A}_{b11} &= -\mathcal{A}_{b22} = -\sin(2(a+\gamma))\sin 2\beta\cos\theta \\
\mathcal{A}_{b12} &= \mathcal{A}^*_{b21} = e^{i2\alpha}(i\cos(2(a+\gamma)) - \cos 2\beta\sin(2(a+\gamma)))\cos\theta \\
\mathcal{A}_{b13} &= \mathcal{A}^*_{b31} = ie^{-i(2a-\alpha+\gamma)}\sin\beta\sin\theta \\
\mathcal{A}_{b23} &= \mathcal{A}^*_{b32} = ie^{-i(2a+\alpha+\gamma)}\cos\beta\sin\theta \\
\mathcal{A}_{b33} &= 0,
\end{aligned} \tag{B.3}$$

where * denotes complex conjugation,

$$\begin{aligned}
\mathcal{A}_{c11} &= -\mathcal{A}_{c22} = -(-1 + (\cos^2\theta + 1)\cos^2\beta)\cos 2b \\
&\quad + \cos(2(a+\gamma))\cos\theta \sin 2\beta \sin 2b \\
\mathcal{A}_{c12} = \mathcal{A}^*_{c21} &= e^{i2\alpha}(\sin 2b \cos\theta(\cos(2a+2\gamma)\cos 2\beta + i\sin(2a+2\gamma)) \\
&\quad + \frac{1}{2}\cos 2b \sin 2\beta(\cos^2\theta + 1)) \\
\mathcal{A}_{c13} = \mathcal{A}^*_{c31} &= e^{-i(a-\alpha)}(-\sin 2b \sin\beta e^{-i(a+\gamma)} + \cos 2b \cos\beta \cos\theta e^{i(a+\gamma)})\sin\theta \\
\mathcal{A}_{c23} = \mathcal{A}^*_{c32} &= -e^{-i(a+\alpha)}(\sin 2b \cos\beta e^{-i(a+\gamma)} + \cos 2b \sin\beta \cos\theta e^{i(a+\gamma)})\sin\theta \\
\mathcal{A}_{c33} &= -\cos 2b \sin^2\theta
\end{aligned}$$

$$\mathcal{A}_\phi = \begin{pmatrix}
-\frac{1}{\sqrt{3}}(1 - 3\sin^2\theta\cos^2\beta) & -\frac{\sqrt{3}}{2}e^{2i\alpha}\sin 2\beta \sin^2\theta & \frac{\sqrt{3}}{2}\cos\beta e^{i(\alpha+\gamma)}\sin 2\theta \\
-\frac{\sqrt{3}}{2}e^{-2i\alpha}\sin 2\beta\sin^2\theta & -\frac{1}{\sqrt{3}}(1 - 3\sin^2\theta\sin^2\beta) & -\frac{\sqrt{3}}{2}\sin\beta e^{-i(\alpha-\gamma)}\sin 2\theta \\
\frac{\sqrt{3}}{2}\cos\beta e^{-i(\alpha+\gamma)}\sin 2\theta & -\frac{\sqrt{3}}{2}\sin\beta e^{i(\alpha-\gamma)}\sin 2\theta & \frac{1}{2\sqrt{3}}(1 + 3\cos 2\theta)
\end{pmatrix}. \tag{B.4}$$

Bibliography

[1] P. Weinberg, M. Bukov, L. D'Alessio, A. Polkovnikov, S. Vajna, and M. Kolodrubetz. Adiabatic perturbation theory and geometry of periodically-driven systems. *Physics Reports*, 688:1–35, 2017. ISSN 0370-1573. doi:https://doi.org/10.1016/j.physrep.2017.05.003. Adiabatic Perturbation Theory and Geometry of Periodically-Driven Systems.

[2] P. M. Schindler and M. Bukov. Counterdiabatic driving for periodically driven systems. *Phys. Rev. Lett.*, 133:123402, Sep 2024. doi:10.1103/PhysRevLett.133.123402.

[3] A. Patra and C. Jarzynski. Classical and quantum shortcuts to adiabaticity in a tilted piston. *The Journal of Physical Chemistry B*, 121(15):3403–3411, 2017. doi:10.1021/acs.jpcb.6b08769. PMID: 27700088.

[4] R. Barends, A. Shabani, L. Lamata, J. Kelly, A. Mezzacapo, U. L. Heras, R. Babbush, A. G. Fowler, B. Campbell, Y. Chen, Z. Chen, B. Chiaro, A. Dunsworth, E. Jeffrey, E. Lucero, A. Megrant, J. Y. Mutus, M. Neeley, C. Neill, P. J. J. O'Malley, C. Quintana, P. Roushan, D. Sank, A. Vainsencher, J. Wenner, T. C. White, E. Solano, H. Neven, and J. M. Martinis. Digitized adiabatic quantum computing with a superconducting circuit. *Nature*, 534(7606):222–226, June 2016. ISSN 1476-4687. doi:10.1038/nature17658.

[5] M. Bukov, L. D'Alessio, and A. Polkovnikov. Universal high-frequency behavior of periodically driven systems: from dynamical stabilization to floquet engineering. *Advances in Physics*, 64(2):139–226, March 2015. doi:10.1080/00018732.2015.1055918.

[6] P. M. Schindler and M. Bukov. Geometric floquet theory. 2025. doi:10.48550/arXiv.2410.07029.

[7] D. Sels and A. Polkovnikov. Minimizing irreversible losses in quantum systems by local counterdiabatic driving. *Proceedings of the National Academy of Sciences*, 114(20):E3909–E3916, 2017. doi:10.1073/pnas.1619826114.

[8] A. Graf and F. Piéchon. Berry curvature and quantum metric in n-band systems: An eigenprojector approach. *Phys. Rev. B*, 104:085114, Aug 2021. doi:10.1103/PhysRevB.104.085114.

[9] M. Kolodrubetz, D. Sels, P. Mehta, and A. Polkovnikov. Geometry and non-adiabatic response in quantum and classical systems. *Physics Reports*, 697:1–87, 2017. ISSN 0370-1573. doi:https://doi.org/10.1016/j.physrep.2017.07.001. Geometry and non-adiabatic response in quantum and classical systems.

[10] M. Byrd. The geometry of su(3). 1997. doi:10.48550/arXiv.physics/9708015.

[11] A. Pais and V. Rittenberg. Semisimple graded lie algebras. *Journal of Mathematical Physics*, 16(10):2062–2073, 10 1975. ISSN 0022-2488. doi:10.1063/1.522421.

[12] R. Hermann. *Lie Groups for Physicists*. The mathematical physics monograph series. Benjamin, 1966.

[13] G. Khanna, S. Mukhopadhyay, R. Simon, , and N. Mukunda. Geometric phases for su(3) representations and three level quantum systems. *Annals of Physics (New York)*, 253(1), 01 1997. doi:10.1006/aphy.1997.5601.

[14] B. B. Zhou, P. C. Jerger, V. O. Shkolnikov, F. J. Heremans, G. Burkard, and D. D. Awschalom. Holonomic quantum control by coherent optical excitation in diamond. *Phys. Rev. Lett.*, 119:140503, Oct 2017. doi:10.1103/PhysRevLett.119.140503.

[15] N. V. Vitanov, A. A. Rangelov, B. W. Shore, and K. Bergmann. Stimulated raman adiabatic passage in physics, chemistry, and beyond. *Rev. Mod. Phys.*, 89:015006, Mar 2017. doi:10.1103/RevModPhys.89.015006.

[16] P. Knight and P. Milonni. The rabi frequency in optical spectra. *Physics Reports*, 66(2):21–107, 1980. ISSN 0370-1573. doi:https://doi.org/10.1016/0370-1573(80)90119-2.

[17] E. J. Meier, K. Ngan, D. Sels, and B. Gadway. Counterdiabatic control of transport in a synthetic tight-binding lattice. *Phys. Rev. Res.*, 2:043201, Nov 2020. doi:10.1103/PhysRevResearch.2.043201.

[18] H. Zhou, Y. Ji, X. Nie, X. Yang, X. Chen, J. Bian, and X. Peng. Experimental realization of shortcuts to adiabaticity in a nonintegrable spin chain by local counterdiabatic driving. *Phys. Rev. Appl.*, 13:044059, Apr 2020. doi:10.1103/PhysRevApplied.13.044059.

[19] A. A. Abdumalikov Jr, J. M. Fink, K. Juliusson, M. Pechal, S. Berger, A. Wallraff, and S. Filipp. Experimental realization of non-abelian non-adiabatic geometric gates. *Nature*, 496:482–485, 2013. doi:10.1038/nature12010.

[20] F. N. Ünal, A. Bouhon, and R.-J. Slager. Topological euler class as a dynamical observable in optical lattices. *Phys. Rev. Lett.*, 125:053601, Jul 2020. doi:10.1103/PhysRevLett.125.053601.

[21] J. Zhang, T. H. Kyaw, S. Filipp, L.-C. Kwek, E. Sjöqvist, and D. Tong. Geometric and holonomic quantum computation. *Physics Reports*, 1027:1–53, 2023. ISSN 0370-1573. doi:https://doi.org/10.1016/j.physrep.2023.07.004. Geometric and holonomic quantum computation.

[22] D. A. Lidar, I. L. Chuang, and K. B. Whaley. Decoherence-free subspaces for quantum computation. *Physical Review Letters*, 81(12):2594–2597, September 1998. ISSN 1079-7114. doi:10.1103/physrevlett.81.2594.